SAN FRANCISCO DISTRICT
U.S. ARMY CORPS OF ENGINEERS

AIRBORNE REMOTE SENSORS APPLIED TO ENGINEERING GEOLOGY AND CIVIL WORKS DESIGN INVESTIGATIONS

BY
RONALD H. GELNETT
Principal Investigator

UNDER
NATIONAL AERONAUTICS AND SPACE ADMINISTRATION
Contract No. 160-75-89-03-10, SRT PROJECT 122
DECEMBER 1975

SAN FRANCISCO DISTRICT
U.S. ARMY CORPS OF ENGINEERS

AIRBORNE REMOTE SENSORS APPLIED TO ENGINEERING GEOLOGY AND CIVIL WORKS DESIGN INVESTIGATIONS

BY
RONALD H. GELNETT
Principal Investigator

UNDER
NATIONAL AERONAUTICS AND SPACE ADMINISTRATION
Contract No. 160-75-89-03-10, SRT PROJECT 122
DECEMBER 1975

CONTENTS

FIGURES

PLATES

ACKNOWLEDGMENTS

This work was authorized by the U.S. Army Corps of Engineers, Office of the Chief of Engineers (OCE), and partially funded by the National Aeronautics and Space Administration under Contract No. 160-75-89-03-10, SRT Project 122. In addition to the Satellite imagery, NASA also flew and provided several types of photography and thermal infrared imagery. The author is indebted to Messrs. J. Jarman and D. Penick of OCE, and O. Smistad and F. Neuman of NASA, as well as others in both agencies.

Special thanks are due Major George Baena, Commanding Officer of the 184th Military Intelligence Company (Aerial Surveillance), Fort Lewis, Washington, and the many officers and enlisted men who flew and provided the side-looking airborne radar imagery of the study area under contract to the District.

Further appreciation is extended to Colonels James L. Lammie and Charles R. Roberts, District Engineers of the San Francisco District, U.S. Army Corps of Engineers, for their constant encouragement in this as well as many other remote sensing projects, and to Mr. H.E. Pape, Jr., Chief of the Engineering Division, and Mr. N. Shimizu, Chief of the Foundations and Materials Branch, for their support. Gratitude is expressed to a number of Corps geologists who assisted in the geologic mapping and groundtruth investigations of the study area, and in particular Mr. Ted Coffman, Project Geologist on the Butler Valley Dam and Reservoir Project.

Credit is also due Motorola Aerial Remote Sensing, Inc., Phoenix, Arizona, for providing the time and funds to complete and print this report.

I. INTRODUCTION

This study was authorized and approved by NASA in June, 1972. Its purpose is to assist the Corps of Engineers in determining the usefulness of various airborne remote sensing systems in the detection and identification of regional and specific geologic structural features that may affect the design and location of engineering structures on major civil works projects.

Careful consideration of both regional and local geologic features are important to the designer of major engineering structures, such as dams, nuclear power plants, tunnels, underground installations, highways and railroads, etc.; because they can have a significant effect on the stability and economics of the project. In some cases, geologic factors are instrumental in determining the location and type of structure to be constructed. The identification and evaluation of these factors are the responsibility of the engineering geologist.

Geologic factors of fundamental importance to the design engineer and engineering geologist on dam and reservoir projects are:

(1) Physical properties and characteristics of the geologic formations in the foundation, abutments, spillway and outlet works, reservoir area, and along routes of relocated roads and transmission lines;

(2) Orientation, pattern and condition of faults, fractures, joints bedding planes, cleveage and schistocity in foundation areas, cut slopes and tunnel routes;

(3) Stability of reservoir wall rocks;

(4) Proximity of regional faults and shear zones;

(5) Regional seismicity; and

(6) Availability of suitability of construction materials.

The Butler Valley Dam and Blue Lake Project was selected as a demonstration site because:

(1) It is located in a remote mountainous region of northern California that is covered by dense evergreen forests;

(2) The regional geology is extremely complex and largely unknown, except for local areas of interest;

(3) The difficulty in deciphering and extrapolating geologic features due to the paucity of exposures; and

(4) It is located in a seismically active region.

This report is an account of the findings derived from the interpretation of various kinds of imagery used in the study area and is supported by considerable groundtruth data in the project area. It is not a concluding thesis on the regional geology, nor are the findings necessarily complete. Future users of the imagery interested in the same or other aspects of the geology in the study area may modify or add to the data reported herein.

Work on the study was initiated and partially completed by the author while employed as Chief Geologist for the San Francisco District, U.S. Army Corps of Engineers, San Francisco, California. Completion was accomplished while an employee of Motorola Aerial Remote Sensing, Inc., Phoenix, Arizona.

II. STUDY AREA

The study area, encompassing about 5,900 square miles (15,280 sq. km.), is located in northern California, approximately 225 miles (363 km.) north-northwest of San Francisco and includes the geologically unique Cape Mendocino area as shown in Fig. 1.

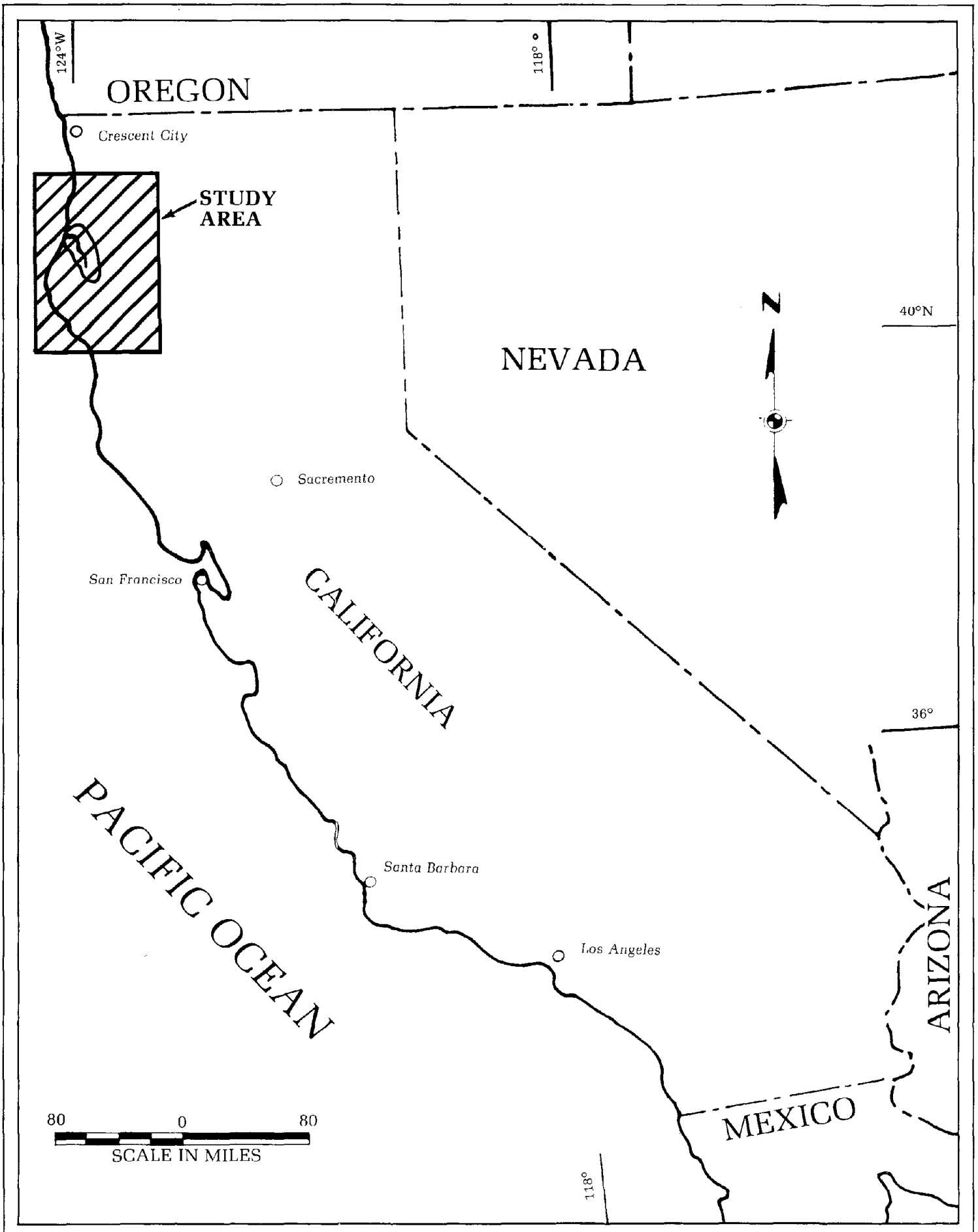

Figure 1. Location Map

Portions of two markedly different geologic provinces are represented within the study area: The Klamath Mountains to the east, and the northern Coast Ranges on the west.

All or parts of five principal drainage basins are within its boundaries; namely, Trinity River, Redwood Creek, Mad River, Van Duzen River and Eel River. The proposed Butler Valley Dam and Blue Lake project is in the northern Coast Ranges province located at river mile 26 on the Mad River, which is near the lower end of an 80-mile long and six-mile wide drainage basin trending northwestward. Consequently, most of the discussions in this report will relate to the geology of the northern Coast Ranges. An oblique aerial view of the dam site, looking east, is shown in Fig. 2.

III. OBJECTIVES

Geologic mapping in the Klamath Mountains is more complete than that of the northern Coast Ranges owing to better exposures, discriminate lithologic units, and less severe structural deformation. In contrast, much of the geologic mapping in the northern Coast Ranges is of a reconnaissance nature depicting a generalized northwest lithic and structural regional trend. This is not because of a lack of interest by geologists, but rather due to the complexity of the geology, poor exposures which account for somewhat less than ten percent of the land area, and the dense forest cover. Hence, the construction of regional geologic maps necessarily requires liberal use of inferences and extrapolation, and some interpolation.

Corps geologists compiled a substantial amount of geophysical and geological data during three field seasons of subsurface exploration and mapping in the immediate vicinity of the project area. Refinements to published geologic maps were made, a number of small, previously unmapped faults trending in a northeast and north-south

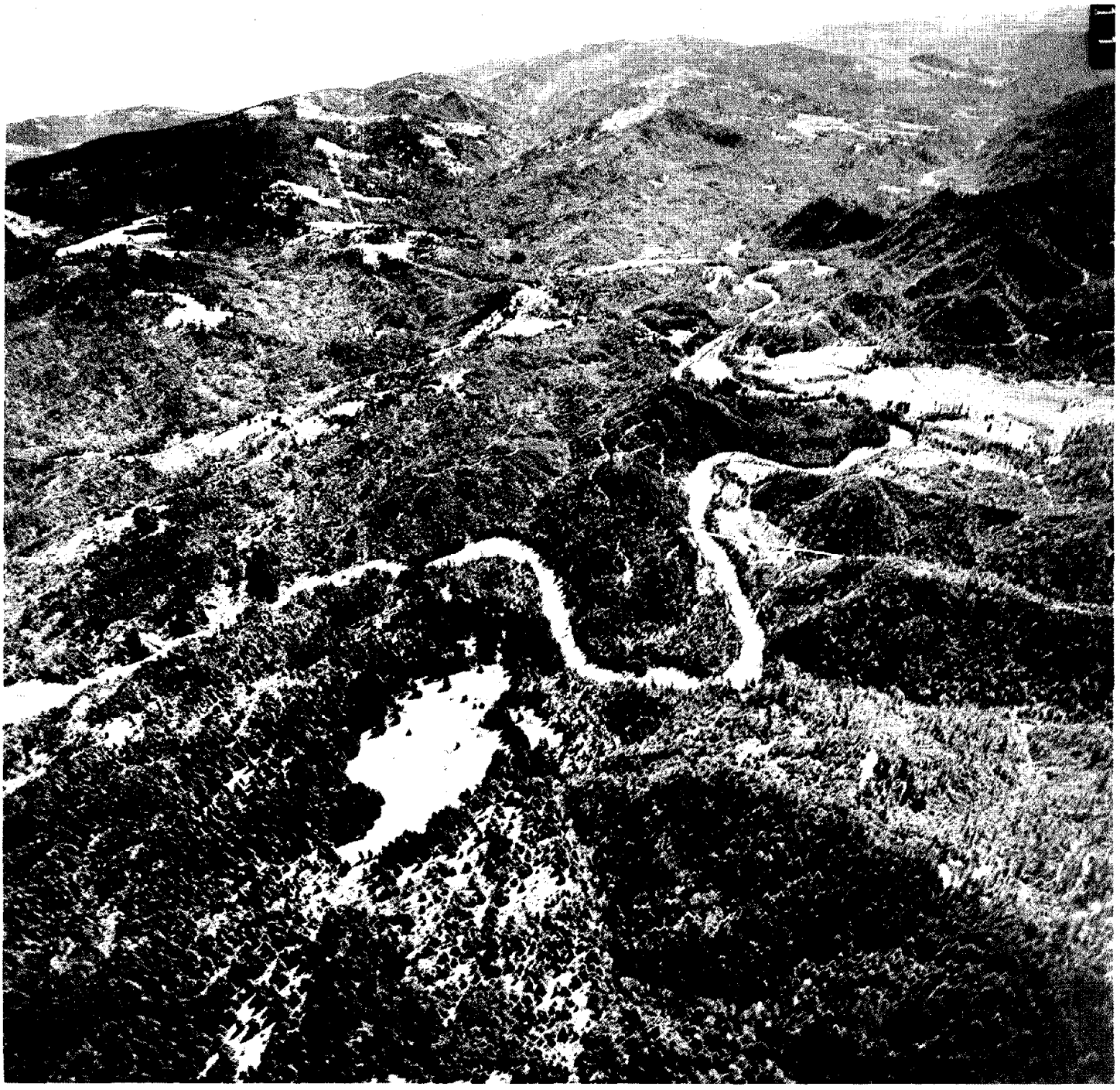

Figure 2. Oblique air photo of dam site and reservoir, looking east.

direction were discovered, and many of the geologic factors affecting the foundation design of the dam, spillway and outlet works were ascertained. Yet little improvement was made in determining the regional structural fabric due to the difficulty in tracing rock units and faults from one stream course to another.

Since the region is known to be seismically active, a number of questions needed to be answered, such as: (1) Were the faults in the project area local or part of a regional pattern? (2) Were the inferred major faults traversing the region continuous, active or inactive? and (3) Were there as yet undiscovered major faults in the region that may affect the design of the structures? Secondly, numerous landslides were mapped along the northeast side of the reservoir area where the relocated road is planned. However, their upper limits and boundaries are indistinct due to the amount of overburden materials, tree cover and erosion. Accordingly, the dense tree cover made it difficult at best to define the above features from the interpretation and use of multiple-scale (1:9,000 to 1:33,600) color air photos acquired for the project. To perform detailed regional geologic mapping, or to drill every area of uncertainty, would be economically impracticable.

In an attempt to help resolve some of the above problems in a cost-effective and time-efficient manner, the District sought the support of the U.S. Army and NASA to conduct a comprehensive remote sensing survey using side-looking airborne radar, thermal infrared line scanning, and high-altitude multiband photography. Specific objectives were fourfold:

(1) To identify and refine the location of major regional faults and possibly detect previously unknown faults;

(2) To ascertain the presence or absence of a regional fault and fracture pattern that may be related to that found locally in the vicinity of the project;

(3) To assist in defining the landslides along the proposed relocated road; and

(4) To evaluate the applicability of the various sensor systems for future use by other engineers and geologists.

IV. GEOLOGIC SETTING

Plate 1 presents the regional geology over most of the study area as published by the California Division of Mines and Geology in the 1:250,000 scale Redding Sheet, 1962 edition, Geologic Map of California. It is a compilation of all published and unpublished geological work in this area. As previously stated, portions of two geologic provinces are represented in the study area: the Klamath Mountains to the east and the northern Coast Ranges to the west. A prominent reverse fault dipping NE (Irwin, 1960) separates the two provinces and traverses the study area diagonally from NW to SE along a narrow belt of the pre-Cretaceous schist (ms). This fault over much of its length is parallel to the faults of the San Andreas system. The basis for defining the two provinces is a natural grouping of principal rock units that differ markedly from the standpoint of topography and geologic history.

The principal rock units of the Klamath Mountains range in age from early Paleozoic to late Jurassic and are intruded by batholithic granites. The rock units form general arcuate belts that are concave to the east. Topographically, the province is a rugged mass of mountains with peaks standing from 6,000 to more than 9,000 feet in elevation, side slopes are steep, and the drainage is generally from east to west cutting across the lithic and structural grain of the province.

In contrast, principal rock units in the northern Coast Ranges are chiefly eugeosynclinal rocks, known as the Franciscan Assemblage,

ranging in age from late Jurassic to Cretaceous. There are no granites and no known basement rocks. Both provinces, however, are intruded by abundant ultrabasic rocks. Present evidence (Bailey et. al. 1964) suggests that the entire assemblage may rest directly on a basaltic substratum or peridotite. Topographically, the mountains of the northern Coast Ranges are lower in elevation, generally less than 5,000 feet decreasing toward the coast, and are comprised of a series of ridges separated by V-shaped valleys. Both the lithic and structural grain of the province are conspicuously northwest controlling the drainage which is also northwestward. Slopes are moderate to steep and landsliding is prevalent.

Marine sedimentary rocks of probable late Cretaceous age overlie the Franciscan Assemblage in the Eel River Valley area and near Eureka. Tertiary rocks of Eocene to Pliocene age occur in both provinces. They are chiefly of marine origin in the northern Coast Ranges, whereas they are mainly continental in the Klamath Mountains.

The geologic structure in the study area is highly complex and poorly known particularly in the northern Coast Ranges. The degree of deformation in the rocks in the northern Coast Ranges is much more severe than that of the Klamath Mountains. The arcuate arrangement of lithic belts in the Klamath Mountains is interpreted as resulting from compressive forces from the east, and the boundaries between the lithic belts are chiefly eastward-dipping reverse faults. In contrast, structural features in the northern Coast Ranges appear to have been subjected to changing principal stress directions through east-west to north-south. Major faulting is chiefly normal and reverse, trending to the northwest. An anomalous west-northwest structural trend occurs in the Eel River Valley area near Cape Mendocino as mapped by Ogle, 1953. Smaller faults and shear zones are abundant throughout and trend in a variety of directions.

Recent ideas based upon plate tectonics, or seafloor spreading, attribute the structural complexity of the northern Coast Ranges (melange-style deformation) to the piling-up of oceanic-plate material along a subduction zone associated with a late Mesozoic trench (Ernst, 1970). Looking at the structural trends and the increasing degree of deformation to the east in the northern Coast Ranges, there is a striking appearance of the older rocks having been pressed against the more rigid mass of the Klamath Mountains.

V. SEISMICITY

After Alaska, the Cape Mendocino area, and particularly the area off the coast, is the most seismically active in North America. More than 20 percent of the major historical earthquakes listed for California and Nevada occurred in this area. An important contributing factor to this activity is the San Andreas Fault which is a right-lateral strike-slip fault having from 50 to as much as 350 miles (80 to 564 km.) of relative displacement (Crowell and Walker, 1962, and Hill and Dibblee, 1953). Its age is also not precisely known; some saying as old as late Jurassic and others saying no older than early Miocene. In any event, the San Andreas has long been a prominent feature of the California landscape and has had an unparalleled history of activity extending to this day. See Figure 3 showing the fault and the active area off Cape Mendocino, and Plate 2 showing epicenters of significant historical earthquakes.

More recent studies of the faulting and seismicity in the Cape Mendocino region have revealed additional contributing factors that are of fundamental importance, at least in the late 2 to 5 m.y. (Seeber, 1970; Silver, 1971, et. al.). Figure 4 is a generalized map schematically showing the relationship of the triple junction of three lithospheric plates meeting at Cape Mendocino. They are: the Pacific Plate, the North American Plate,

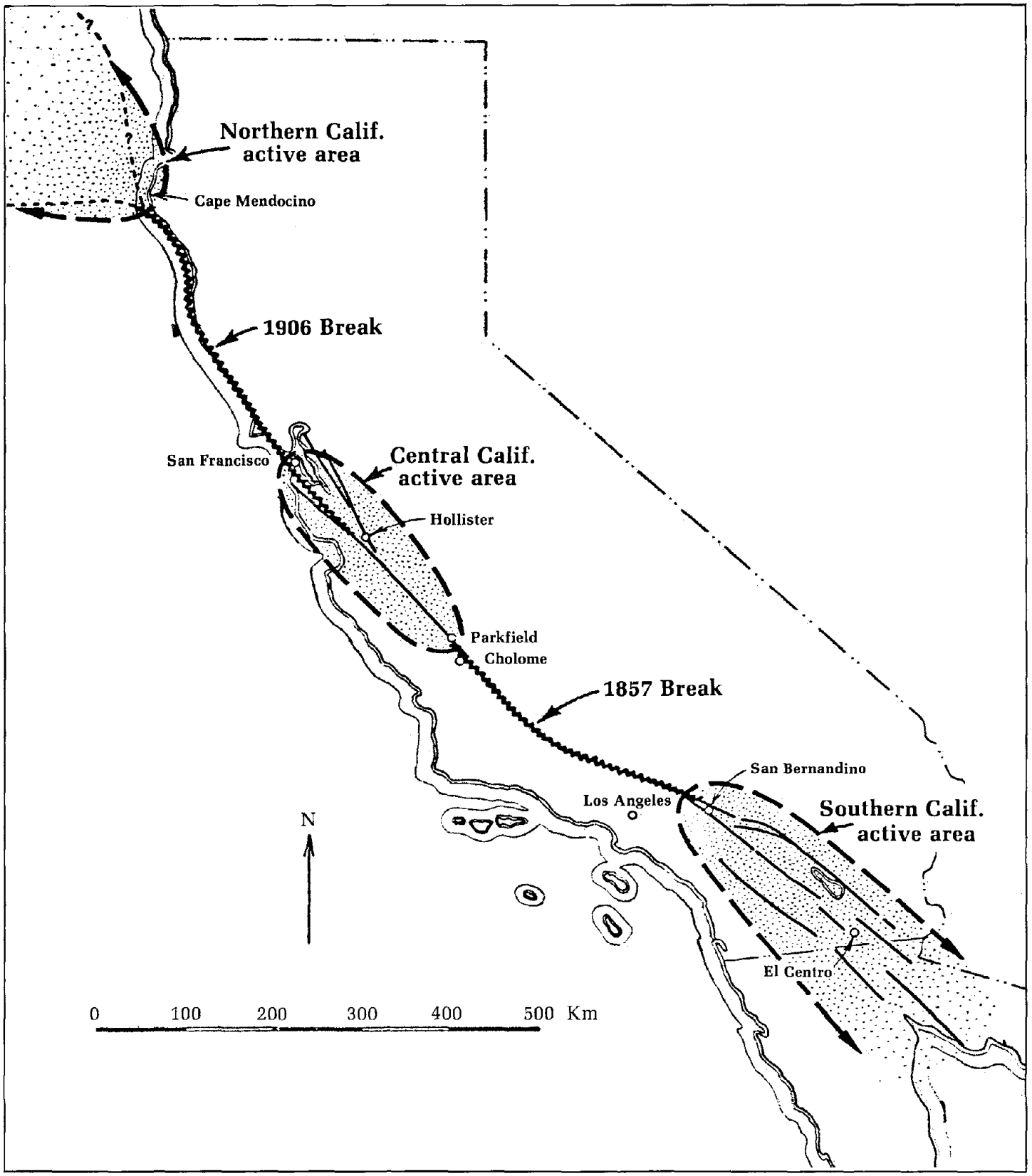

Figure 3. Map of California showing the San Andreas fault with seismic active areas and locations of historic surface breakage. From Allen (1968).

and the Gorda Plate which is here labelled as the Gorda Basin. Subbottom profiling has provided evidence that the San Andreas bends abruptly near Gorda Point, which is just below Cape Mendocino, and merges with the west-trending Mendocino Fault (that portion of the Mendocino Fault between the Gorda Ridge and the Cape is commonly referred to as the Gorda Escarpment).

The basic pattern of relative plate motions at the triple junction requires right-lateral motion on both the San Andreas and Mendocino Faults and underthrusting along the continental margin north of Cape Mendocino. Both Seeber, 1970 and Silver, 1971, present considerable evidence for late Cenozoic internal deformation of the Gorda Basin and underthrusting based on subbottom profiling, microseismic studies, and magnetic anomalies. Several investigations cited internal basin deformation on the basis of earthquake epicenters (Tobin and Sykes, 1968, et. al.). They studied the epicenters in the northeastern Pacific and demonstrated that most earthquake activity is concentrated along the Mendocino Fault, Gorda Ridge, and Blanco Fracture zone.

Dehlinger and others (1967) calculated a block of low-density material underlying the Mendocino Fault from seismic profiling and suggests it is related to underthrusting by the Gorda Plate. Inconclusive but suggestive evidence indicates that the Gorda Escarpment portion of the Mendocino Fault is a reverse fault which could also accommodate appreciable strike-slip motion. Figure 5 is a simplified block diagram of the plate interaction at Cape Mendocino.

Faulting within the Gorda Basin was first inferred to be right-lateral and extending northwestward from Cape Mendocino as shown in Figure 4. Later studies by Silver with subbottom profiling and magnetic anomalies demonstrated that most of the faults in the Gorda Basin trend in a northeast or east-northeast direction paralleled and subparalleled with the Gorda Ridge and lines of weakness associated with SE seafloor spreading, all of which exhibit

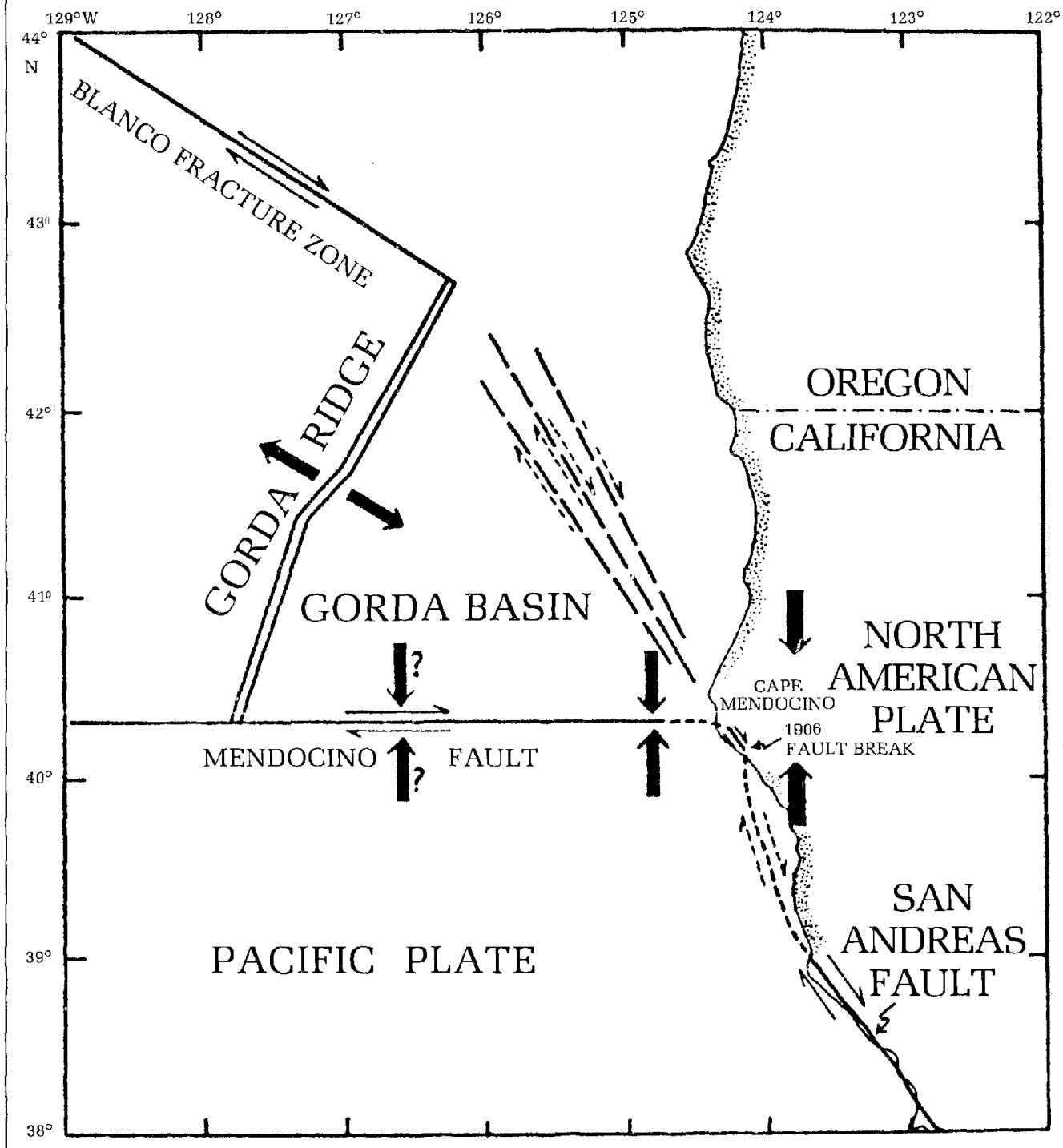

Figure 4. Generalized map of Cape Mendocino area, schematically showing major tectonic features. Dashed heavy lines across Gorda basin are representative of inferred pattern of faulting. Heavy arrows represent regional compression or tension. From Seebar et.al. (1970).

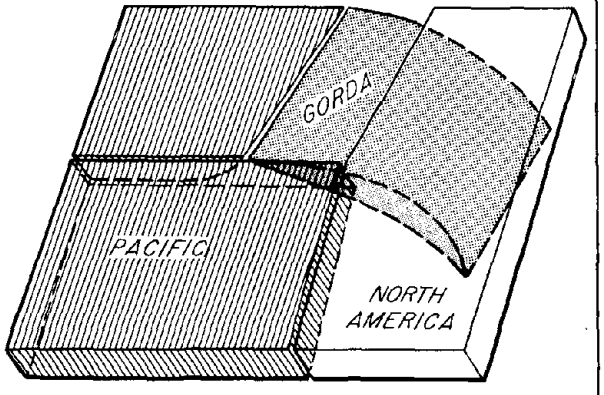

Figure 5. Simplified block diagram of the inferred relationship between the American, Pacific and Gorda lithospheric plates which meet at a triple junction at Cape Mendocino. From E. Silver (1971).

left-lateral movements. The above investigators made three important discoveries: (1) The dextral strike-slip motion along the San Andreas Fault is at present being taken up by similar motion on the Mendocino Fault accompanied by northward thrusting; (2) Right-lateral, left-lateral, and thrusting predominate in the focal mechanism of faulting both on and offshore of Cape Mendocino radiating in east-west, northwest and northeast trends; and (3) earthquake hypocenters are anomalously deeper in the Cape Mendocino area (15 to 35 km.) than anywhere along the San Andreas system to the south.

They suggest the evidence is indicative of a new tectonic regime developing probably in the last 2-5 m.y. in which internal deformation of the Gorda Basin and north-south compression along the Mendocino Fault are important features. This is consistent with historic epicentral locations as they die out rapidly to the north, south and east.

VI. REMOTE SENSORS USED

A. General

Advanced planning and preconstruction exploration and design studies began on the Butler Valley Dam and Blue Lake project in 1966. Imagery from a variety of remote sensing systems were employed on the project, but not all at the same time. Black and white air photos acquired in 1956 and 1966 after the devastating floods in the north coastal region, and multiple-scale color photography acquired in 1970 for topo-map construction in the project and reservoir areas were used extensively throughout the studies.

In 1971, side-looking airborne radar coverage of the study area was flown by the U.S. Army. It was acquired during 1-2

September 1971 and subsequently mosaicked. LandSat-1 (formerly ERTS) satellite imagery of the study became available in the fall of 1972. NASA's P-3 aircraft under the subject SRT contract provided thermal infrared imagery, color infrared and black and white photography in the spring of 1973. High-altitude U-2 aircraft multiband imagery of the project area was also flown by NASA in September 1973.

Since the literature contains abundant data on the LandSat system, thermal infrared line scanning, and certainly metric and multiband photography, only brief descriptions of these sensors are presented herein. Side-looking airborne radar, on the other hand, will be described in more detail because there are a variety of systems in use which are substantially different. Secondly, Radar is unique in that it is an "active" sensor system, whereas all others are "passive."

B. LandSat

NASA's LandSat-1 satellite, launched in a polar orbit at an altitude of 570 miles (918 km.) in July 1972, provided for the first time small scale synoptic views of the earth's surface that stirred universal renewed interest in remote sensing. A single frame scans a 115-mile square (185 km. square) area of the earth's surface at a scale of 1;1,000,000. Each frame is presented in four wavelengths, or bands, covering most of the visible spectrum and a portion of the near infrared--Band 4, 0.5 to 0.6; Band 5, 0.6 to 0.7; Band 6, 0.7 to 0.8; and Band 7, 0.8 to 1.1 micrometers. Reported resolution (groundspot size) of LandSat-1 imagery is 100 meters square.

C. Photography

As stated earlier, multiple-scale aerial photography (B&W, color, color infrared and multiband) was acquired by the Corps and NASA using standard metric and multiband cameras. They are as follows:

1. The District, under contract to private firms, acquired B&W and color metric aerial photos in scales of 1:9,000, 1:12,000, 1:20,000 and 1:33,600;

2. The NASA P-3 aircraft provided 1:24,000 and 1:50,000 scale color infrared and B&W aerial photos; and

3. The NASA U-2 aircraft, in its Vinten-A arrangement, provided multiband aerial photos at a scale of approximately 1:440,000.

Groundspot-size resolution on air photos vary from a few inches to a few feet square (0.1 to 2.0 meters) depending on their scale.

D. Thermal Infrared

The infrared system as configured on NASA's P-3 aircraft is an RS-14 line-scanner manufactured by Texas Instruments. It is also a passive system that detects and measures emitted infrared radiation, but does not depend on reflected solar lighting to obtain the image as with LandSat or aerial photography. Since the amount of infrared energy emitted from any material is affected by its temperature to the forth power, line-scanners are commonly referred to as "thermal infrared" sensors. The RS-14 measures infrared energy in two atmospheric windows; generally referred to as 3 to 5 and 8 to 14 micrometers. Resolution depends on the aircraft altitude and the optical system itself. Groundspot sizes at commonly flown altitudes vary from two to ten feet square (0.7 to 3.0 meters).

A daytime and nighttime flight was planned consisting of two overlapping strips covering the landslide area on the NE side of the reservoir and the saddle dike area just north of the dam site. The objective was to detect soil moisture differences and small seeps to assist geologists in defining landslide

boundaries and fracture traces. However, this mission was unsuccessful due to: (1) Too much tree cover, (2) Extreme relief in the target area; and (3) Aircraft scheduling precluded the nighttime flight. Therefore, no examples are included in this report. Normally, thermal infrared is an excellent sensor for these applications in spite of the fact that it is very time and weather dependent. Experience with the infrared line-scanner in other areas show that the most advantageous time to fly this sensor is between the hours of midnight and sun up.

E. Side-looking Airborne Radar

The Radar imagery of the study area was acquired by the 184th Military Intelligence Company (Aerial Surveillance) under contract to and the direction of the San Francisco District. The system is an APS/94(D) real-aperture (brute force) Radar operating in the 3 cm wavelength (X-Band) region of the electromagnetic spectrum. Radar is called "active" because it generates its own energy to illuminate the earth's surface and operates entirely independent of solar lighting. This fact, coupled with the long wavelength used, means that the Radar antenna can illuminate terrain from any azimuth, day or night, and through cloud cover with controlled illumination (depression) angles. It was designed by Motorola Inc. specifically for the U.S. Army and is mounted on the sophisticated OV-1D Mohawk aircraft.

Unique features of the system are:

1. Near real-time display of the imagery on-board the aircraft.

2. The original film negatives are available for on-the-spot viewing immediately after each flight;

3. The imagery produced is in conventional map scales of

1:250,000, 1:500,000, 1:1,000,000, and 1:2,000,000 while imaging out of the right, left or both sides of the antenna simultaneously; and

4. Changes in aircraft altitude do not alter the mapping scale.

Radar operates on two basic principles: (1) that all materials reflect a portion of the microwave energy transmitted as a pulse from the antenna; and (2) that microwave energy travels in straight lines and at the speed of light. The specialized Radar antenna is fixed to the belly of the aircraft. It transmits a narrow beam of pulsed energy in a perpendicular plane and at an oblique angle to the line of flight. As the aircraft moves forward, the beam scans the terrain in a series of rapid sequential pulses. Energy reflected from the ground to the receiving antenna is transformed into optical energy and is exposed on photographic film. The film records at a rate proportional to the ground speed of the aircraft to maintain the proper map scale.

Thus, the imagery strip is comprised of thousands of data lines per inch, each line recording discrete variations in high and low intensity returns differentiated as various shades of gray: light grays for high reflected Radar energy returns and darker grays for low reflected Radar energy returns. The amount of reflected energy is primarily a function of: (1) topography, (2) angle of incidence between the radiated beam and the reflecting surface, (3) surface roughness (angular vs. specular), (4) moisture content, and (5) dielectric constant of the reflecting material.

The resulting Radar image looks much like a small scale low sun-angle aerial photograph because of the shadows, but the two are entirely different. With Radar you are viewing the terrain as the reflected microwave energy portrays it and not as the

eye would see it in the visible spectrum. It is essential that the interpreter understands these differences.

Unlike other Radar systems and aerial sensors having fixed focal lengths or fields of view, the map scale of the imagery in this Radar system remains constant at all aircraft altitudes because it is a time-distance function of the microwave pulse. However, the elevation of the Radar illumination (pseudo sun angle) does vary with changing aircraft altitudes and, accordingly, so does the amount of shadow (no return areas) on the imagery.

The look direction and proper amount of shadowing are probably the two most important factors in geological applications of Radar. Too much or too little shadow results in significant loss of data. Since the investigator can control the look direction, or azimuth, and vertical angle of illumination, judicious use of them provides him with the ability to accentuate geological features in any type of terrain, flat lying or mountainous. Radar is particularly effective in areas of heavy forest cover as will be demonstrated in the examples of this report.

Resolution of Radar imagery is a commonly misunderstood term and is not related to the conventional minimum ground-spot size as in photographic resolution. Radar resolution is defined as the "minimum separation" between two targets (artillery, trucks, tanks, etc.) that will appear individually on the imagery as measured in the "range direction" (perpendicular to the aircraft) and in the "azimuth direction" (parallel with the line of flight). In unclassified Radar systems, these dimensions vary from 15 to 200 meters. That does not mean that an object or feature has to be that big before you can see it on Radar. Linear features for example, such as, roads, railroads, power lines, etc., and geological features, such as, dikes, faults, ridges, creeks, etc., of substantially smaller dimensions are

clearly visible and routinely identified on Radar because of sequential pulse recording. Thus, if high reflective (hard) targets are excluded, conventional ground-spot size resolution for Radar imagery could be generally stated as less than ten meters.

VII. DISCUSSION OF RESULTS

A. General

Imagery from the various remote sensor systems used, interpretive results, and discussions herein pertain to geological applications only. Use of the same imagery for other applications could diverge substantially from these findings. Use of remote sensor imagery on this project, or any other project, must not be considered as a final, definitive answer to geological exploration and related problems. Similarly, there is no one sensor system that will provide all the answers. No such all-encompassing method currently exists or is likely to be developed. However, remote sensing methods are valid and can be economically important in that: (1) some geological features can be readily identified which cannot be detected in any other way, or that are often overlooked in the field, and (2) knowing where to concentrate groundtruth efforts can save substantial man-months or man-years of field work. Their use on this project added materially to and improved significantly upon existing knowledge of the regional and project area geology.

All of the imagery examples contained herein are of high quality and represent the best samples obtained with the various remote sensors used. Understandably, due to the printing process, all are now fourth-generation lithographic prints, except for Plate 3 (Radar mosaic) which is a 1.9X reduction and sixth-generation print.

The objectives of this study relate primarily to identifying fault and fracture patterns, which the imagery interpreter must necessarily regard as lineaments until groundtruth examinations are made. Thus, it is important to describe them and their occurrence.

B. Lineaments

Lineaments and their closely related synonyms (fracture traces, microfractures, mesofractures, megajoints, photolinears, etc.) have been noted on air photos and topographic maps for almost a century (Hobbs, 1911, Lattman, 1958, and Blanchet, 1957). Most of the investigators of lineaments relate their definitions to the length of the feature, which necessarily is governed by the scale of the imagery or map used. The term "lineament" is preferred by this author because the exact cause is unknown. A lineament can be a fault, joint, fracture, shear zone, or zones of increased frequency of any of them as observed in the rock unit itself, or the trace of these features propagated to the surface through substantial thicknesses of younger rocks or overburden materials. Once it has been specifically identified in the field as a joint, fault or shear zone, then it is, of course, no longer a lineament.

Lineaments identified on airborne imagery appear as naturally occurring, comparatively straight or slightly curved features usually accentuated by erosion. The most common are topographic alignments, drainage alignments, and tonal variations in soils or vegetation, or combinations of the three. Since lineaments are approximately straight alignments that transect a variety of local geologic features, the majority of them must extend nearly vertically with depth.

Consistent, worldwide, roughly orthogonal fracture and joint patterns have been recognized in the Precambrian Shield areas and basement rock bodies of most continents. The basic shear

set consists of components oriented in the NW, NE, NS and EW directions. The causative mechanism is not well understood, but most agree their origin is related to global tectonics. Similar patterns have been observed in the overlying sedimentary rocks and alluvium, which were apparently inherited from the basement rocks as the surface pattern is consistent with their basic shear set (Hodgson, 1961). Again, the propagating mechansim is not agreed upon, but the repeated diurnal stresses caused by earth tides is believed to be an important contributing factor because they have been observed in unconsolidated sediments and glacial till (Rumsey, 1971).

C. Project Geology

Rocks underlying the project area are portions of two principal formations; the Franciscan Assemblage of late Jurassic to Cretaceous age, and the Falor Formation (named by Manning and Ogle, 1950) of mid-Pliocene age shown as Kjf and Tm, respectively, on Plate 1 and in Figure 12b. Franciscan rocks are comprised of a heterogenous assemblage of indurated sandstones (graywackes), shales, altered volcanics (greenstones), and lesser amounts of serpentinite, chert, schist and conglomerate. The Falor Formation consists of unconsolidated marine sediments that were deposited in a shallow arm of the sea in mid-Pliocene time. These sediments are chiefly poorly cemented sands, clays and siltstones containing lenses of pebble conglomerates.

The Franciscan rocks were intensely faulted and tightly folded in late Cretaceous time and subsequent periods of uplift and faulting. The Falor sediments are only mildly deformed by comparison and a portion of them have been down faulted into the Franciscan along NW-trending normal faults of late Pliocene age and thereby preserved from erosion. Estimated displacement along the western boundary fault is about 1,000 feet (308 meters). Manning and Olge, 1950, mapped a number of NE-trending faults which transect and offset the NW-trending boundary faults. Their age is thought to be related to the Plio-Pleistocene

faulting in the northern Coast Ranges. There is no evidence of recent activity on any of the faults.

1. Formation boundaries

Foundations for the dam, spillway, and outlet works are entirely within the more resistent Franciscan rocks, consisting of thick-bedded graywackes and thinly interbedded shales and graywackes which strike N 70°-80° W and dip 50° to 65° NE. Figure 6 is a medium-scale air photo of the dam site, north being toward the ~~bottom~~ right. The conspicuous hairpin bends in the river can be used as a reference in the other sample imagery. The Mad River flows from left to right in this view. Also note the contrasting topography on either side of the river, better illustrated in Figures 7 and 12a.

Previous investigators in this area mapped the late Jurassic and Cretaceous rock units as simply Franciscan, Kjf on Plate 1 and in Figure 12b. In the Eel River Valley area and Coast Ranges to the south, however, Bailey, et. al., 1964, recognized that the younger Franciscan graywackes (Coastal Belt) contained an appreciable amount of K-feldspar and consequently had lower specific gravities, whereas the older Franciscan graywackes (Central and Eastern Belts) rarely contained more than a trace of K-feldspar, had higher specific gravities, and in places were mildly metamorphosed. In the study area the younger and older Franciscan rocks are mapped as K and Kjf, respectively.

Diamond core drilling, sampling and laboratory testing of the graywackes at the dam site revealed a high K-feldspar content, ranging from 16 to 22 percent, and specific gravities averaging about 2.54--lower than the 2.65 to 2.70 for the older Franciscan graywackes. Suggesting that

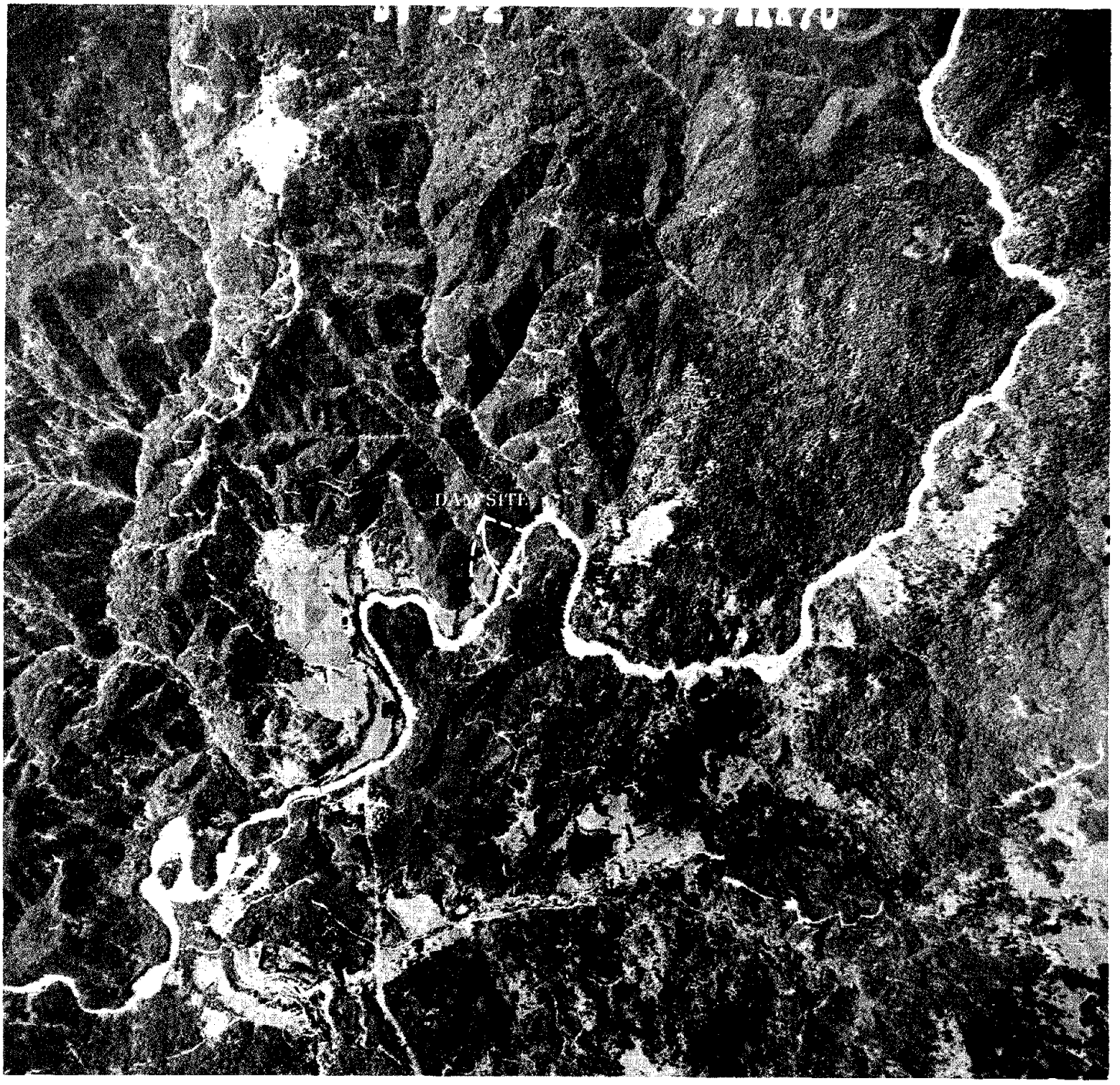

Figure 6. Vertical air photo of dam site. *Scale 1: 40,000*
(Corps of Engineers)

these rocks may be in fact younger Franciscan (K) rocks. In outcrops, which are almost entirely limited to the banks of the river, these graywackes could be traced for several miles upstream along the west side of the reservoir. The exact boundary of this rock unit was not mapped by Corps geologists and probably could not map it because of the dense tree cover and lack of exposures at higher elevations.

The approximate boundary of this rock unit can be interpreted from the anomalous topographic configurations on photos, Figures 7a and 7b; LandSat, Figure 9; and Radar, Figures 12a and 13a. In comparing these images, note the difference in definition between the Red and Infrared Bands in Figures 7, 8 and 9. The Red Bands, or visible spectrum, portrays the area more like the naked eye sees it and the vegetation is overpowering, particularly in Figure 8. Whereas the Infrared Bands, or nonvisible spectrum, tend to suppress the effect of the vegetation making topographic features more distinct. Experience with the different bands, photographs and LandSat, consistently demonstrate this relationship for areas with heavy forestation. Similarly, constructing color composites of LandSat Bands 4, 5 and 7 only compounds the vegetation effect. However, quite the reverse is true in sparsely vegetated or nonvegetated areas. Topographic and geologic features show up better in the Red Bands.

Radar, as previously described, portrays terrain in a unique manner accentuating topographic and geologic features equally well in vegetated or nonvegetated areas, Figures 12a and 13a. Note that the imagery scales of the photos, Figure 7, and the Radar are the same: 1:250,000, and how clearly the subject rock unit boundary is displayed. The sun elevation on the LandSat image is 21 degrees, and the average illumination (depression) angle on the Radar, at mid-range, is 17 degrees. The Radar image was acquired

from an aircraft altitude of 16,500 feet m.s.l. (5 km.), looking east through 50 percent cloud cover.

Vegetation detail is suppressed in Radar because the returns are integrated into common shades of gray. It does not penetrate or strip the vegetation from the terrain as commonly believed. To illustrate, the sharp but broken north-south line (about 0.6 inches, or 1.5 cm, long) in the upper center of Figure 13a, on a west-facing slope, is a property line separating a logged-off field to the east from the standing trees on the west. And just above this line, on a north-facing slope, is a rectangular area that was logged off several years ago. Here, the replanted trees are partially grown up which the Radar return clearly indicates.

2. Landslide area

The landslide area bordering the eastern margin of the reservoir (Figure 7a), across which the proposed relocated road is to be constructed, was mapped in the field and the upper limits drilled and sampled. This work revealed that the area is underlain at a shallow depth by sheared Franciscan rocks, principally shales and serpentinite, and that it is an area of numerous active landslides which coalesce in their lower portions. The landslides are of concern to the design engineer for two primary reasons: (1) stability of the relocated road, culverts, and bridges along the route, and (2) the possibility that the changed conditions created by the reservoir waters along the lower portions might reactivate old landslides or accelerate movement on active ones resulting in a loss of reservoir storage space, or perhaps create waves that could damage boat docks in recreation areas.

The U-2 photograph, Figure 7a, and particularly the Radar image, Figure 13a, indicated that the entire area might be

Scale 1:250,000

Figure 7a. NASA U-2 vertical air photo; near IR Band (690-760 nm) taken 27 Sept. 1973.

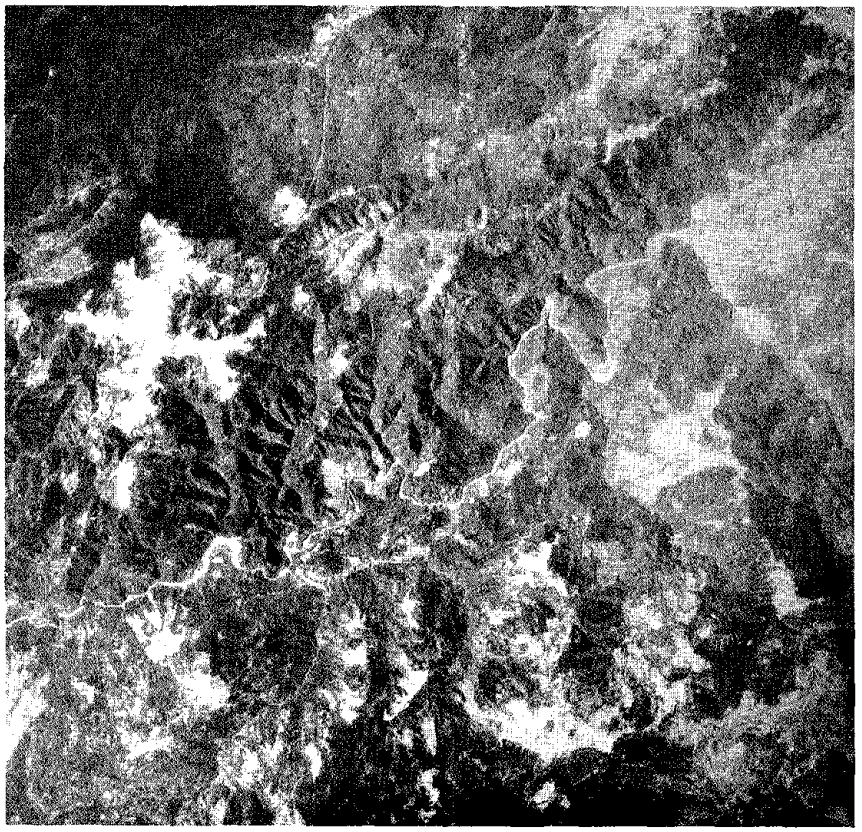

Figure 7b. NASA U-2 vertical air photo; Red Band (580-680 nm) taken simultaneously with figure 7a on 27 Sept. 1973.

Scale 1:250,000

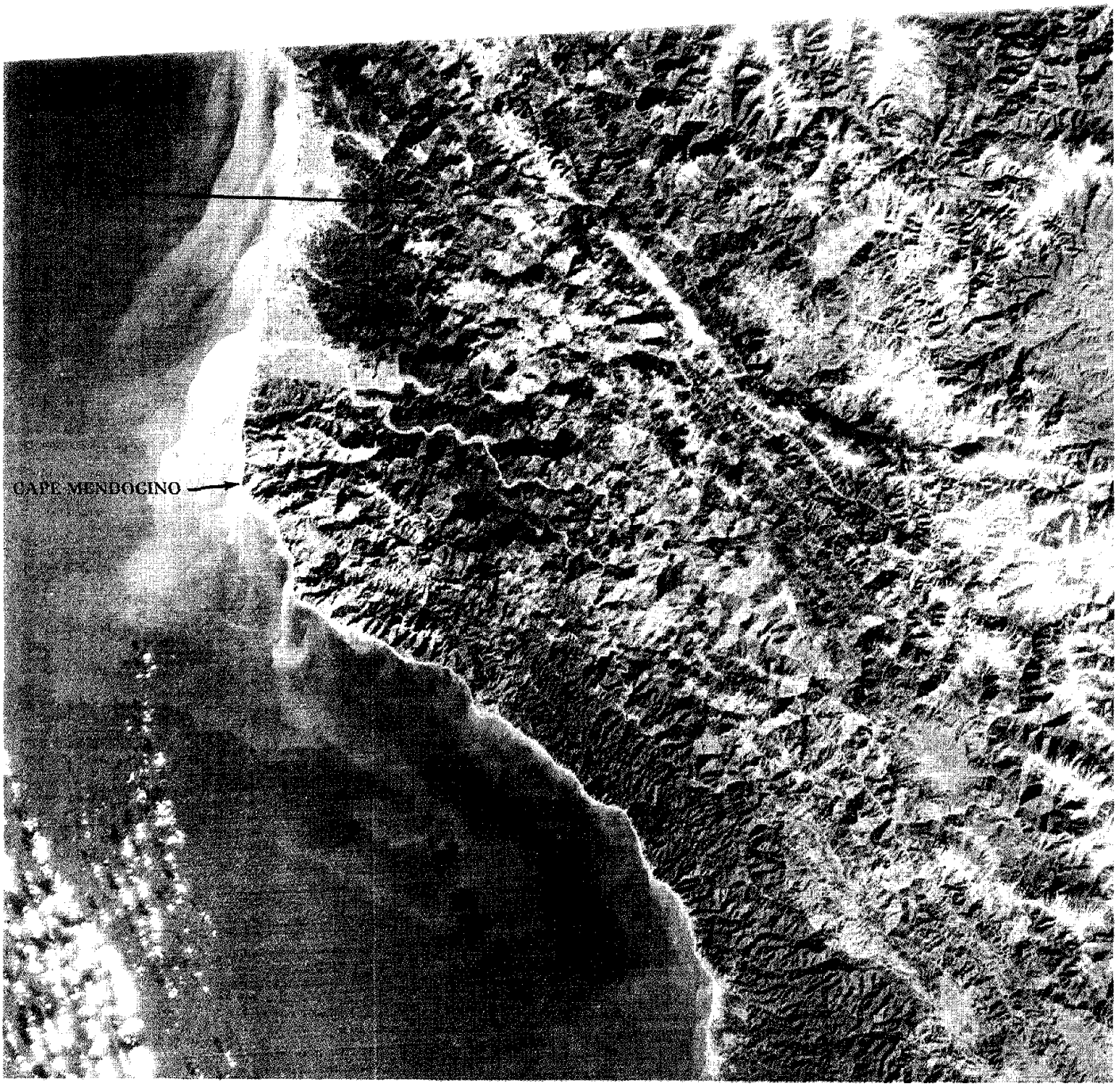

Figure 8. NASA, Landsat-1 Band 5 image of Cape Mendocino area with sun elevation of 21 degrees, 1 January 1974.

Scale 1: 1,000,000

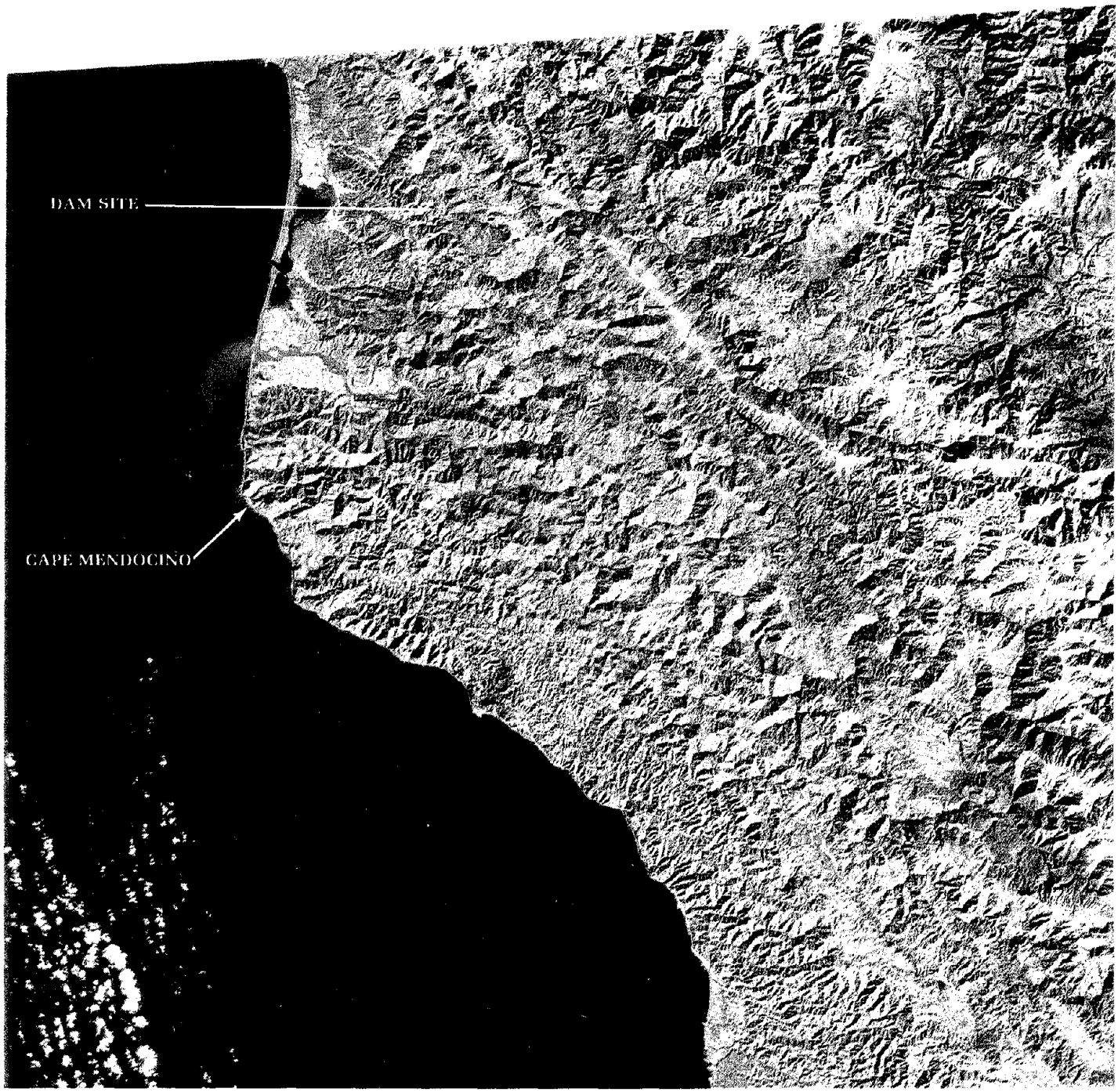

Figure 9. NASA, Landsat-1 Band 6 image of Cape Mendocino area with sun elevation of 21 degrees, 1 January 1974.

Scale 1: 1,000,000

an integrated mass of landslides instead of a number of individual slides. Substantial tree covered areas separate the active slide areas which supported only grass and sparse vegetation. Subsequent and on-going field work suggested that this was probably a correct interpretation. Most of the tree covered areas exhibited diagnostic features of ancient, presently stable, slides, and the obvious active portions were grass covered.

3. Mapped and unmapped faults

Manning and Ogle, 1950, in the course of their Master's thesis field work during the summer of 1947 on the Blue Lake Quadrange, were the first to recognize and map NE-trending faults in this region, right hand one quarter of Figure 12b. Rich, 1973, interpreted from LandSat imagery a number of NE-trending lineaments in the study area, Figure 10. The author also interpreted a striking number of prominent lineaments from the Band 6 LandSat image, Figure 9, which appear to converge on Cape Mendocino, Figure 11.

Early exploration and geologic mapping at the dam site by Corps geologists revealed three sets of local faults with trends to the NW, NE, and NS. The previously mapped major faults, separating the Falor from the Franciscan rocks to the north and the Freshwater Fault to the west, with minor modifications, were found to be essentially as mapped. The NW and NE set of local faults at the dam site predominate, are reasonably tight, and dip vertically through 60 degrees NE, and 80 degrees NW, respectively. They exhibit normal displacements. All of the NS-trending faults, much smaller than the NW or NE faults, have extremely sharp contacts, strike between north and N 10^{o} E, and dip consistently toward the east at angles of 45 to 50 degrees. Relative displacements could not be ascertained due to

overburden cover. Although the trends of the mapped local faults clearly transect the narrow ridges in the project area, they could not be conclusively traced from one side to the other due to the lack of exposures and tree cover.

Interpretation of the subsequent imagery revealed a striking number and persistent set of NE-trending lineaments in the project area and the entire study area as well. This discovery could be of fundamental importance to both the project and the understanding of the regional structural geology, which will be discussed later. Viewing the project area and entire study area in light of the information interpreted from the imagery, substantially changed the perspective of the regional structural geology. Faults mapped during prior field work were reinvestigated, prominent lineaments examined for the possibility of faulting, and the age relationship of NE vs. NW faulting evaluated.

The reader is again invited to closely study Figures 6, 7, 8, 9, 13 and 14 for a comparison of the various kinds of imagery from the standpoint of identifying geologic structural features. A capsulated summary is as follows: (1) the high resolution of the conventional air photo shows too much detail and has a limited field of view to adequately detect the trends of these features; (2) the small scale of the U-2 multiband photos with their larger field of view and choice of Bands provides substantially more information, but vegetation is a hindrance; (3) the LandSat images are of too small a scale and low spatial resolution to yield local definition, yet gross lineaments of considerable length are clearly evident by the integration of topographic, drainage, and tonal features; and (4) it is obvious that Radar provides far more definition on both local and regional geologic structural features.

Lineaments of three kilometers or greater are plotted in Figure 13b. Note that four principal trends are present

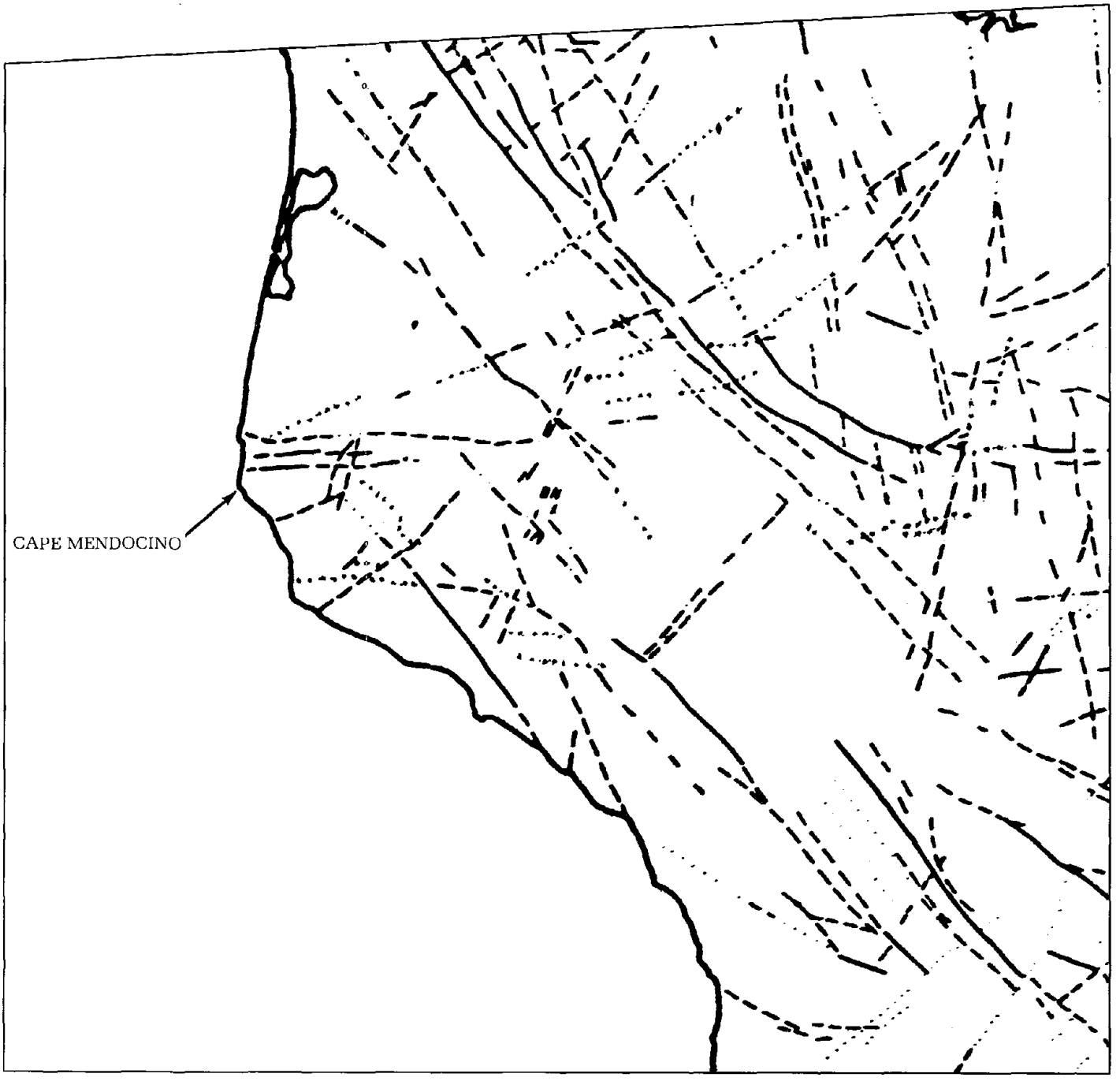

Figure 10. Lineaments interpreted from Landsat-1 imagery, after Rich (1973).

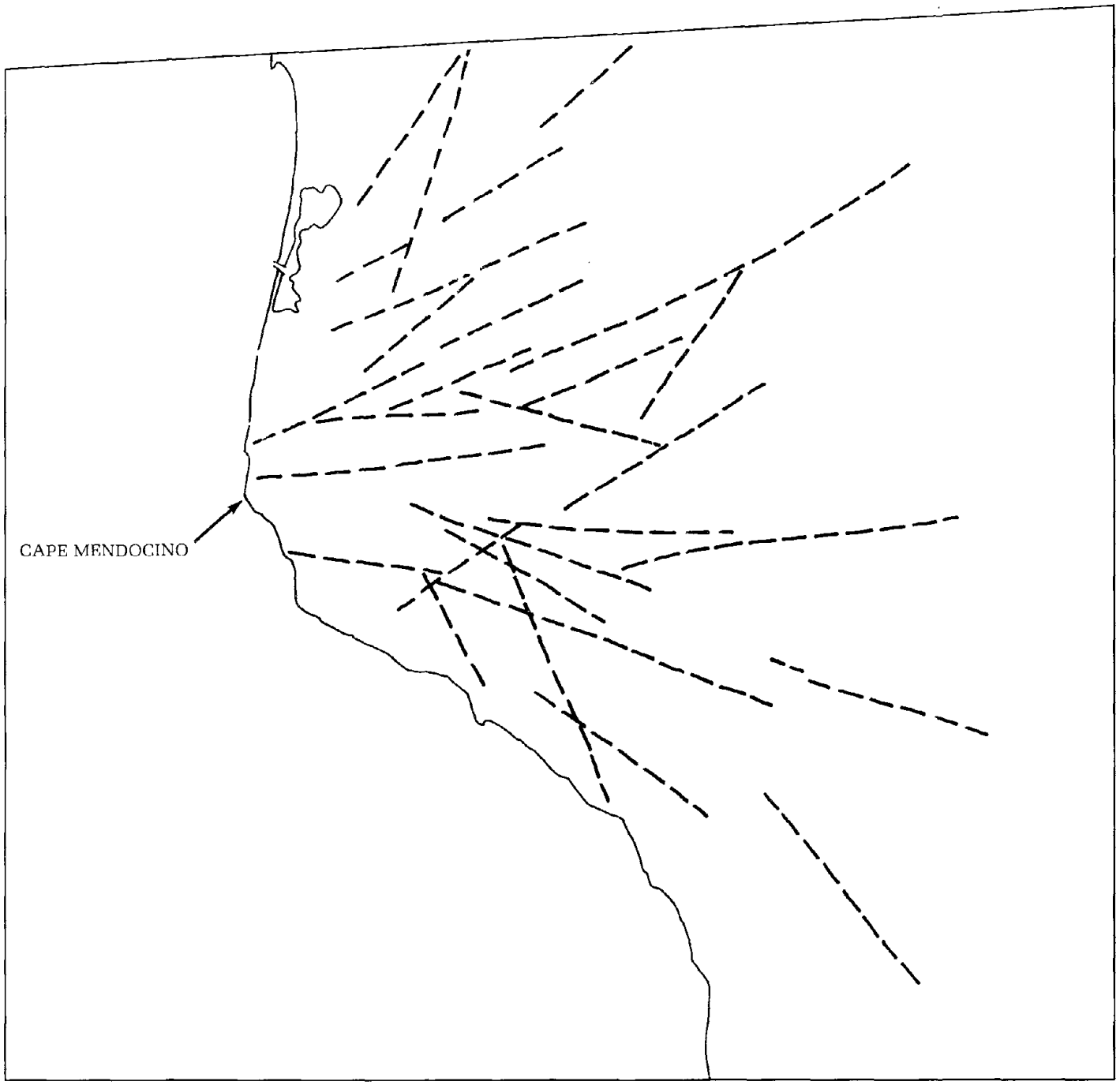

Figure 11. Converging trend of major lineaments in the Cape Mendocino area. Complementary lineament sets purposely omitted.

Scale 1: 1,000,000

and that the NW, NE and NS faults mapped at the dam site do indeed conform to the regional pattern. Known bedding trends or hogbacks and cultural features such as roads, property lines and transmission lines, etc., are carefully excluded. It should be emphasized here that all lineaments are not faults. Those unfamiliar with photo interpretation are often quick to equate lineaments to faults to activity to earthquakes. In fact, in most other regions of the country, only a very small percentage turn out to be faults--most are fractures with no observable displacement. However, knowing the intense deformation and pervasive faulting in the Franciscan Assemblage, a higher percentage of the mapped lineaments can be expected to be faults or shear zones.

Lineaments verified in the field as faults, or interpreted from the imagery as probable faults based on offset topographic and drainage features, are shown in Figure 14b. The faults in the immediate vicinity of the dam site were carefully checked in the field. Most of these faults were identified during prior field work but their extent and trends were poorly known. However, one prominent fault of 10 kilometers in length, marked by arrows in the extreme right side of Figure 14b and in Figure 7a, was repeatedly overlooked in the field. Note the N 10° E trend.

4. Freshwater Fault

The faults at the dam site are partially covered by Pleistocene and Holocene terrace deposits. Dozer trenches, cut through these terrace deposits to the bedrock, were examined in detail for possible desplacements. All were found to pre-date the terraces, indicating their inactivity. The Freshwater Fault, however, eight miles (13 km) west of the dam site, is the closest major fault believed to be active. The northern extension has been observed to

displace Pleistocene deposits and the epicenter of a strong earthquake measuring 6.6 on the Richter Magnitude Scale (21 Dec 1954) was located in the vicinity of its trace, see Plate 2. The design engineer must necessarily know or have reasonable estimates on the distance between his structure and the causative fault, the magnitude of the maximum creditable earthquake that could be expected from future activity along this fault, and the direction from which the energy will be coming in order to incorporate appropriate safety factors in the design of the structure.

In accessing the maximum magnitude, consideration is given to the mapped length of the fault as it is related to the amount of energy that can be expected in future earthquakes. Published maps (Plate 1) show the Freshwater Fault to be approximately 42 miles (68 km) in length, which is major by most standards. If it is continuous over its entire length, it is reasonable to assign a high magnitude value to this fault. Ogle, 1953, states that the Freshwater Fault is probably post-Cretaceous in age with several thousands of feet of displacement, although he did not observe the fault plane in the field. Most of the evidence for its location is based on the approximate boundary between upper Cretaceous (Ku) rocks and Franciscan (Kjf) rocks.

The boundary between these formations is evident on the Radar (Fig. 14) from the anomalous topography and closely approximates the trace of the fault as mapped. However, the SE half of the fault is obliterated by a complex set of what can be interpreted as faults. If this evidence, derived from the Radar imagery, can be substantiated in the field, the assignment of the maximum creditable earthquake on the Freshwater Fault may be higher than need be, unnecessarily taxing the economics of the project.

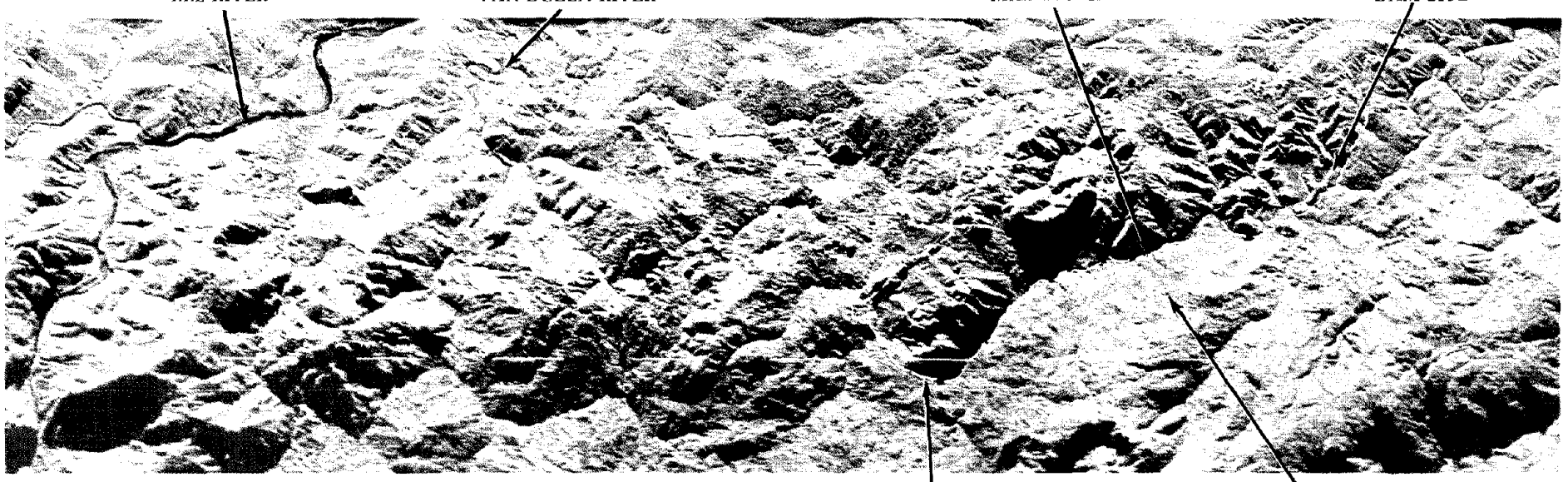

Figure 12a. Radar strip of project area, at taking scale of 1:250,000 (U.S. Army)

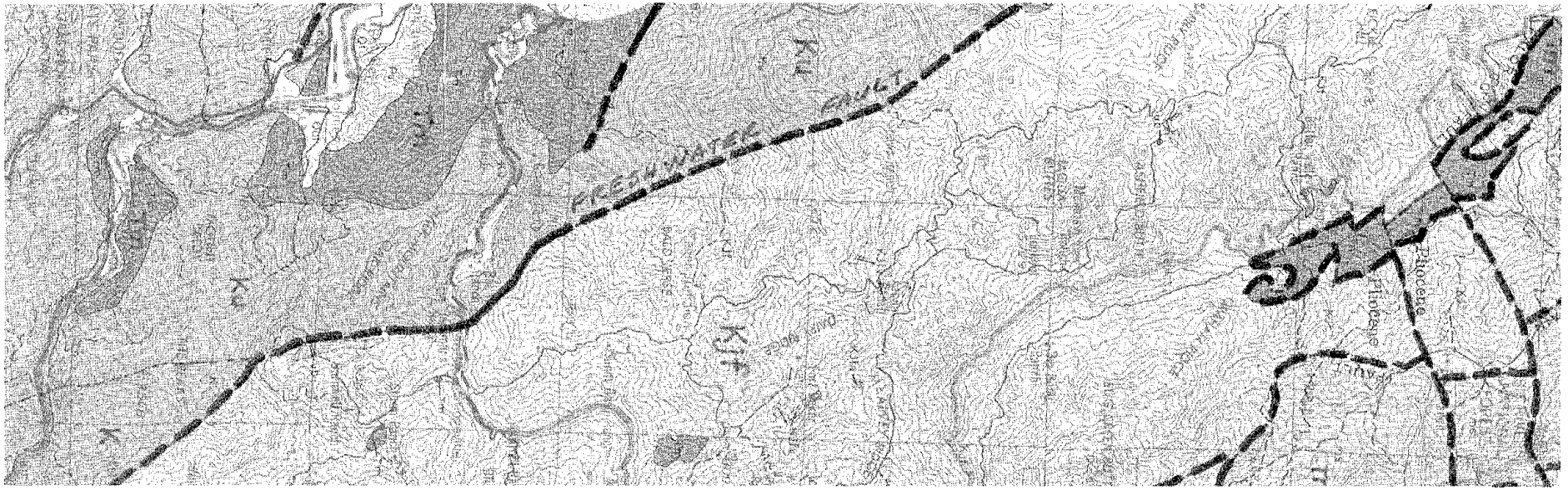

Figure 12b. Geologic map of project area; State of California, Redding Sheet (1962).

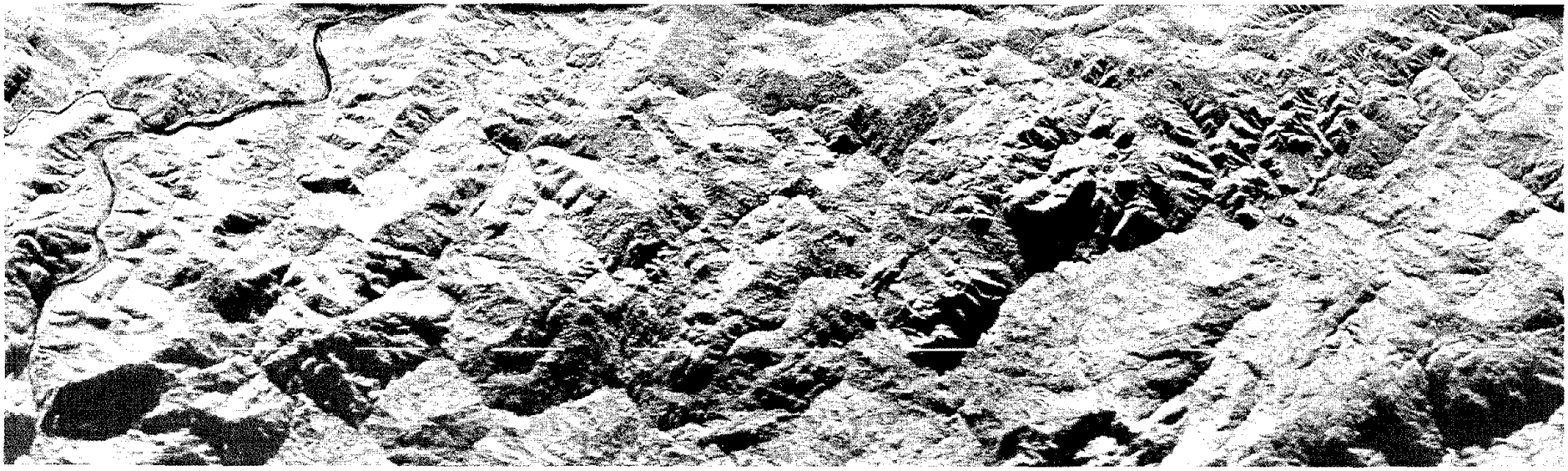

Figure 13a. Radar strip of project area, at taking scale of 1:250,000 (U.S. Army)

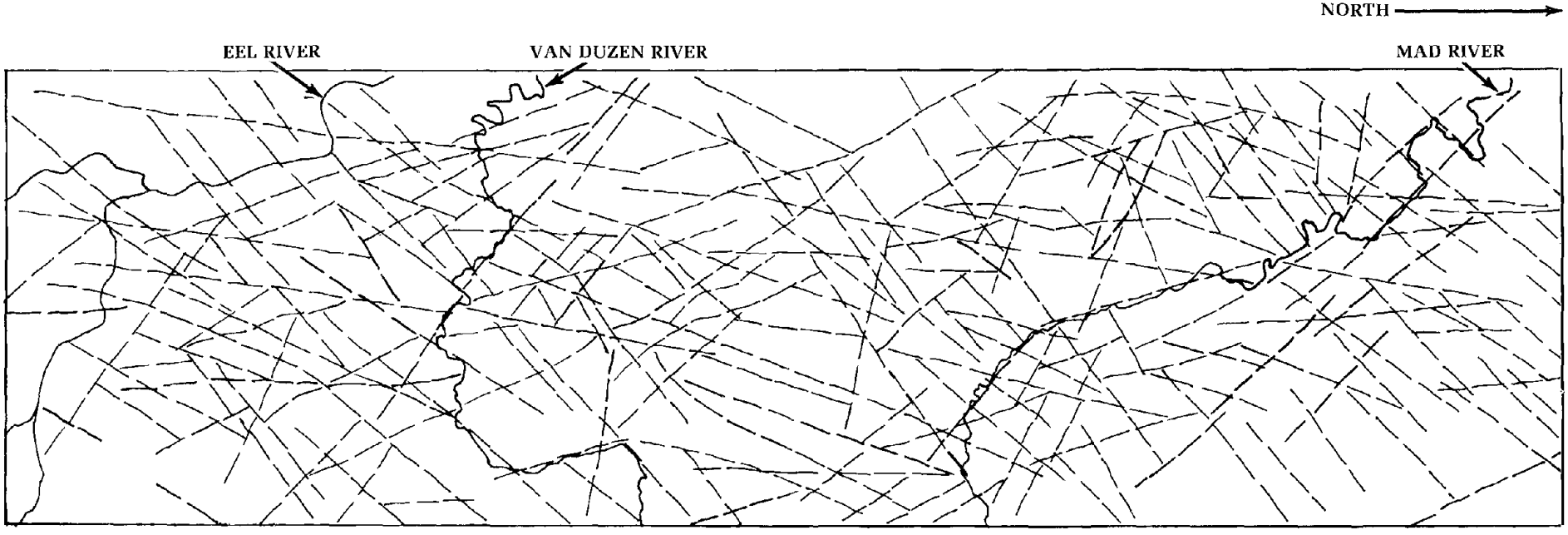

Figure 13b. Principal lineaments interpreted from Radar (figure 13a).

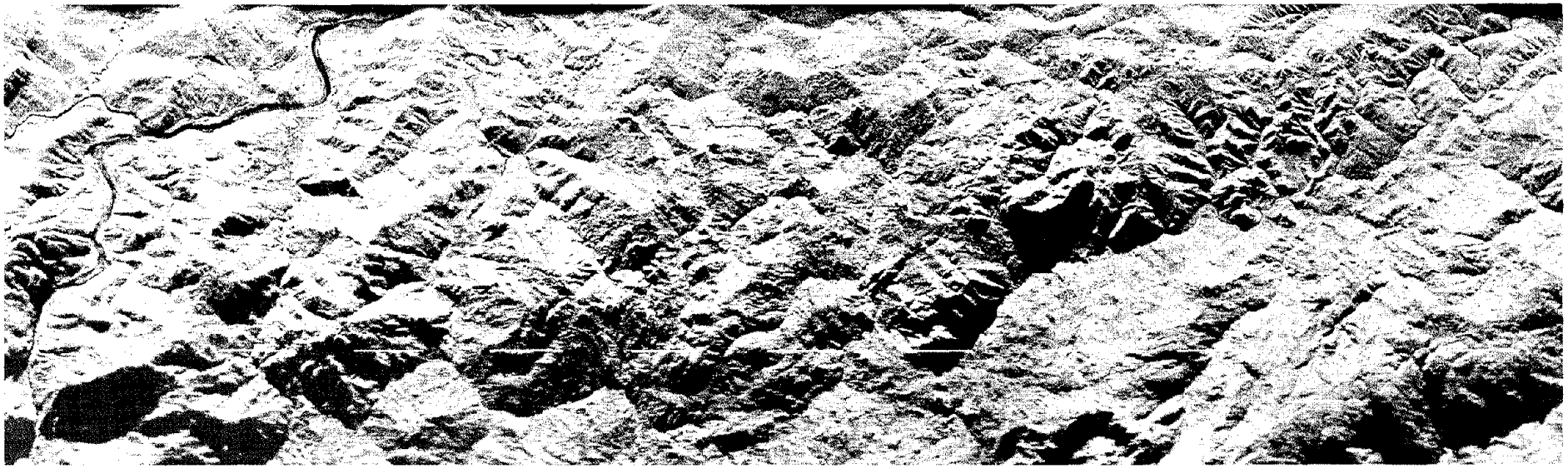

Figure 14a. Radar strip of project area, at taking scale of 1:250,000 (U.S. Army).

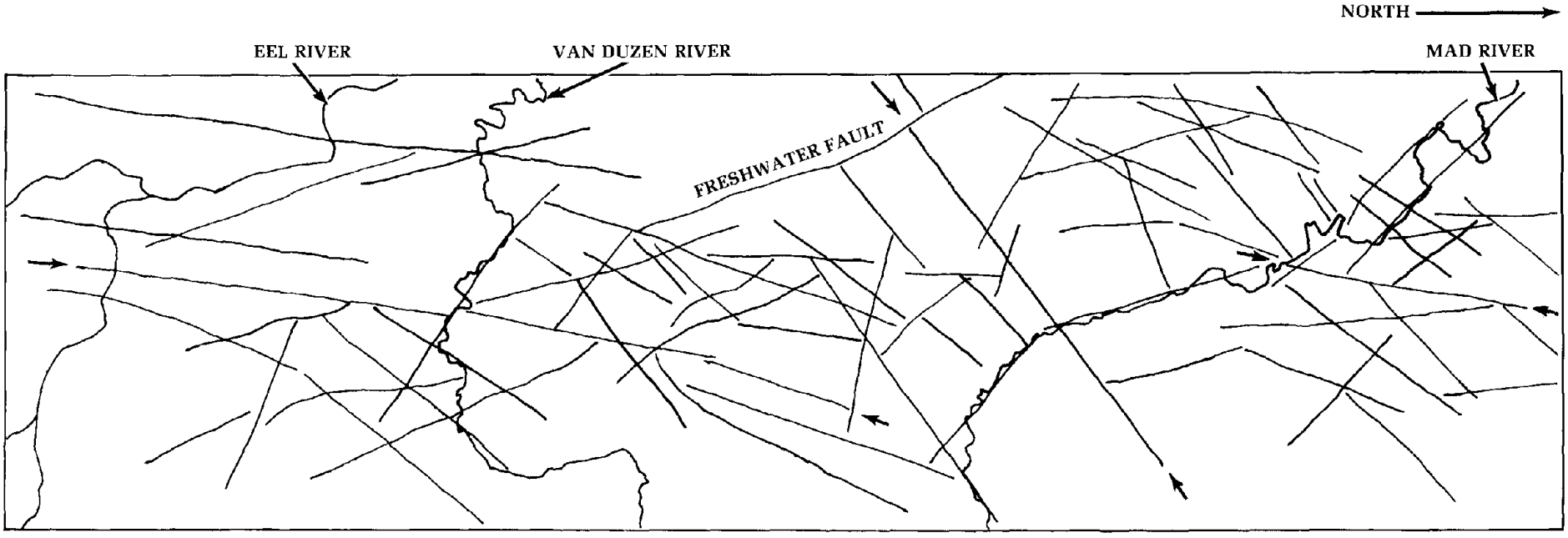

Figure 14b. Lineaments mapped or interpreted as probable faults; arrows mark most prominent.

D. Regional lineament pattern

In the process of determining the regional lineament pattern in the study area, the author interpreted U-2 photographs, Radar, and a number of different LandSat images. As previously mentioned, the near infrared region was found to provide the best structural detail. In spite of the repetative coverage by the satellite, a surprisingly few frames were cloud free. It was also apparent that the winter scenes, having the lowest sun elevation, provided more structural information. However, due to the small scale and comparatively low resolution of LandSat images, lineaments of less than about eight miles (13 km) in length were questionable, whereas lineaments of 30 or more miles (48 km) were readily apparent due to the gross integration of aligned ridges and drainage courses. Although some of these are obvious structural features, caution must be exercised, because upon closer inspection of larger scale imagery there is no apparent reason or suggestive evidence of a structural discontinuity. Ironically, the excellent quality and high resolution of the U-2 photographs portrayed too much detail. Tree cover was particularly distracting. In contrast, lineaments portrayed on Radar, as has been demonstrated, are clearly evident and in better detail.

Plate 3 is a Radar mosaic constructed from 12 north-south strips of 1:250,000 scale imagery. A constant aircraft altitude of 16,500 feet m.s.l. (5 km) was maintained and the look direction is to the east. Side lap between strips averaged 55 percent. The mosaic herein is a sixth-generation print of about 1.9X reduction. Lineaments were interpreted from positive transparancies of individual Radar strips and the mosaic at the original scale. Since the primary objective was to determine the regional structural fabric, only lineaments of five kilometers or greater

in length were mapped. Cultural features and known bedding trends or hogbacks were carefully excluded. Coordinates of the end points of each lineament are determined on the digitizer and put on magnetic tape for computer plotting. To avoid erroneous azimuths on those lineaments that have curved traces, they were broken into straight line segments. Plate 4 is a reduced computer plot of the resulting lineaments. The study area includes 1242 lineaments of 5 to 45 kilometers in length. Note the contrasting lineament density between the northern Coast Ranges and Klamath Mountains provinces.

Reducing this information to a useful form in which meaningful evaluations can be made is accomplished by constructing rose diagrams or histograms. Histograms are particularly useful for plotting lineaments because the unit cell (azimuth interval) can be readily varied to refine the data. The histogram plot of the lineaments in the study area is shown in Figure 15. Azimuths in degrees occur along the bottom (north is 0, west is -90, and east is 90) and the number of lineaments in each azimuth cell is recorded along the right and left. A 3-degree azimuth cell is shown here. The bisector of the various groupings is called the "point of central tendency" which represents the average trend for that group of lineaments. Here they are: N 42^{o} W, N 3^{o} E, N 36^{o} E, and N 65^{o} E. They form two sets of N 42^{o} W and N 36^{o} E, and N 3^{o} E and N 65^{o} E which are separated by 78^{o} and 62^{o}, respectively. In other areas where the rocks have not undergone such severe deformation or that are underlain by basement rocks, these peaks are substantially more well defined.

The surprising result of this analysis--or not so surprising considering the complex compressive stresses that have affected this area--is that 59 percent of the lineaments are in the northeast quadrant and most prominent in the N 36^{o} E group. The amount of east-west crustal shortening in the

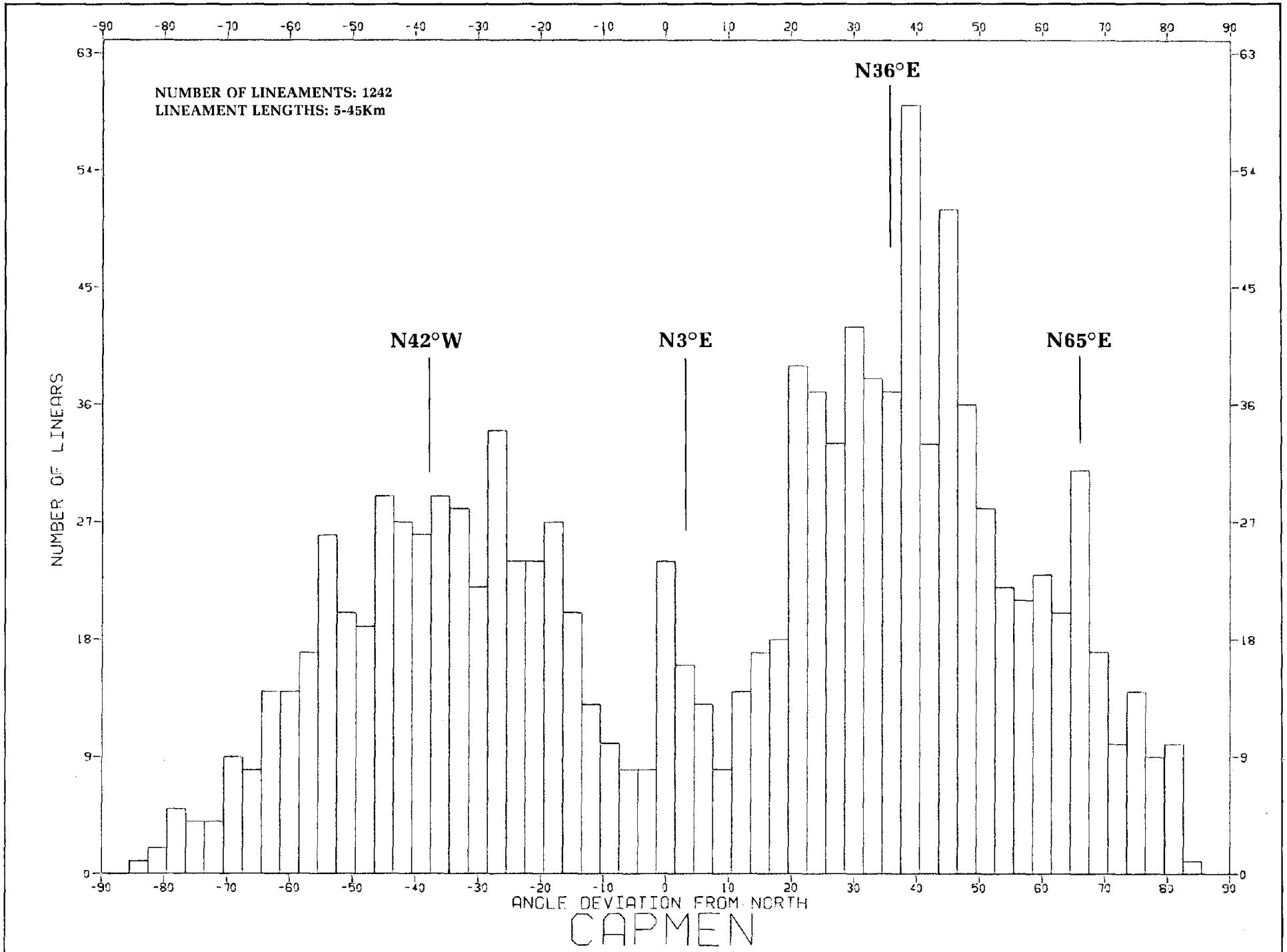

Figure 15. Lineament Histogram.

northern Coast Ranges with associated northwest faulting and, more recently, the interaction of the previously mentioned triple-junction of the lithospheric plates at Cape Mendocino, logically requires a conjugate set of shears or fractures. Secondly, the lineament trends closely approximated the trends of local faults mapped in the project area.

VIII. CONCLUSIONS

The purpose of this study is to assist engineering geologists and engineers in determining the applicability of airborne remote sensing systems in the detection and identification of geological features that may affect the design of the Butler Valley Dam and Blue Lake Project. Primary objectives are:

(1) To refine the location of known regional faults and possibly detect previously unknown faults;

(2) To determine the presence or absence of a regional fault and fracture pattern that may be related to that found locally in the vicinity of the project;

(3) To assist in defining landslides existing along the proposed relocated road; and

(4) To evaluate the applicability of individual sensors for future use by other engineers and geologists.

These objectives were satisfactorily achieved, exceeding all expectations. The information obtained from the remote sensor imagery added materially to and improved significantly upon existing knowledge of the geology in the project area as well as the entire

study area. Their use on other engineering projects should be equally rewarding.

Remote sensing methods in themselves must not be considered as a final, definitive answer to geological exploration and related problems. Groundtruth investigations of the interpretive results are imperative, particularly in engineering geological applications. However, use of appropriate sensor systems and proper interpretation of the imagery reveal important geological features that may not be identified in any other way. Secondly, prudent use of remote sensing methods can be a significant economic advantage. Knowing where to concentrate groundtruth investigations in advance can save several man-years of field work and/or exploration dollars.

Airborne remote sensor coverage in this study is unusually complete; they include (1) multiple scale metric, multiband and infrared photography, (2) thermal infrared imagery, (3) side-looking airborne radar imagery, and (4) LandSat-1 imagery. The application, interpretive results, and concluding remarks herein on the utility of the various kinds of imagery pertain almost exclusively to the detection of geologic structural features in a tree-covered environment. As expected, there is no one sensor system that will provide all of the answers. No such all-encompassing system currently exists or is likely to be developed. Indeed, in the interpretation process, imagery from all of the sensor systems complemented each other nicely.

Relative to the stated objectives, Radar revealed substantially more regional and local geologic structural detail than any of the other systems. Radar's ability to perceive minute topographic and geologic features lies primarily in its unique format which tends to supress vegetative detail, and its low oblique-illumination angle which accentuates these features. Additionally, the small scale synoptic view of Radar imagery allows the investigator to

recognize discontinuous or intermittent fault traces for what they really are. On large-scale imagery, these features are often misinterpreted or overlooked entirely.

In applying remote sensing methods on future engineering projects, it is doubtful that budgetary limitations would allow the luxury of acquiring all of the above kinds of imagery. In fact, all are not required. Because of the amount of geological detail required in engineering geological applications, the Radar-air photo combination was found to provide the most accurate and complete information. Although most of the subject geologic structural features could not be recognized directly from air photos in this study, they were used extensively to field check the existance and location of features identified on Radar.

IX. SELECTED REFERENCES

Atwater, T., 1970, Implications of plate tectonics for the Cenozoic tectonics of western North America: Geol. Soc. America Bull., v. 80.

Bailey, E.H., Irwin, W.P., and Jones, D.L., 1964, Franciscan and related rocks, and their significance in the geology of western California: California Division of Mines and Geology Bull. 183.

Bailey, E.H., Editor, 1966, Geology of northern California: California Division of Mines and Geology Bull. 190.

Blanchet, P.H., 1957, Development of fracture analysis as exploration method: AAPG Bull., v. 41.

Bolt, B.A., Lomnitz, C., and McEvilly, T.V., 1968, Seismological evidence on the tectonics of central northern California and Mendocino Escarpment: Bull. Seis. Soc. America, v. 58.

Crowell, J.C., and Walker, W.R., 1962, Anorthosite and related rocks along the San Andreas fault, southern California: California Univ. Pubs. Geol. Sei., v. 40.

Curray, J.R., and Nason, R.D., 1967, San Andreas fault north of Point Arena, California: Geol. Soc. America Bull. v. 78.

Dehlinger, P., Couch, R.W., and Gemperle, M., (1967), Gravity and structure of eastern part of the Mendocino Escarpment: Jour. Geophys. Research, v. 72.

Dellwig, L.F., MacDonald, H.C., and Kirk, J.N., 1968, Potential of radar in geological exploration, Proc. 5th Sym. on Remote Sensing of Environment: Univ. of Michigan.

Ernst, W.G., 1970, Tectonic contact between the Franciscan melange and the Great Valley sequence, crustal expression of a late Mesozoic Benioff zone: Jour. Geophys. Research, v. 75.

Hill, M.C., and Dibblee, T.W., Jr., 1953, San Andreas, Garlock, and Big Pine faults, California--a study of the character, history, and tectonic significance of their displacements: Geol. Soc. America Bull., v. 64.

Hobbs, W.H., 1911, Repeating patterns in the relief and in the structure of the land: Geol. Soc. America Bull., v. 22.

Hodgson, R.A., 1961, Regional study of jointing in Comb Ridge-Navajo Mountain area, Arizona and Utah: AAPG Bull., v. 45.

Hodgson, R.A. 1961, Reconnaissance of jointing in Bright Angel area, Grand Canyon, Arizona: AAPG Bull., v. 45.

Irwin, W.P., 1960, Geologic reconnaissance of the northern Coast Ranges and Klamath Mountains, California: California Division of Mines and Geology Bull. 179.

Khain, V.E., and Murator, M.V., 1969, Crustal movements and tectonic structures of continents, in P.J. Hart, ed., The earth's crust and upper mantle: Am. Geophy. Union, Wash., D.C.

Lattman, L.H., and Nickelsen, R.P., 1958, Photogeologic fracture trace mapping in Appalachian Plateau: AAPG Bull., v. 42.

Manning, G.A., and Ogle, B.A., 1950, The geology of the Blue Lake quadrangle, California: California Division of Mines and Geology Bull. 148.

Moore, G.W., 1970, Sea-Floor spreading at the junction between Gorda Rise and Mendocino Ridge: Geol. Soc. America Bull. v. 81.

Ogle, B.A., 1953, Geology of Eel River Valley area, Humboldt County, California: California Division of Mines and Geology Bull. 164.

Podwysocki, M.H., 1974, An analysis of fracture trace patterns in areas of flat-lying sedimentary rocks for the detection of buried geologic structure: NASA-Goddard Space Flight Center Doc. X-923-74-200.

Reeves, R.G., 1969, Structural geologic interpretations from radar imagery: Geol. Soc. America Bull., v. 80.

Rich, E.I., 1973, Relation of ERTS-1 detected geologic structure to known economic ore deposits: Stanford University, unpublished.

Rumsey, I.A.P., 1971, Relationship of fractures in unconsolidated superficial deposits to those in the underlying bedrock: Modern Geol., v. 3.

Seeber, L., Barazangi, M., and Nowroozi, A., 1970, Microearthquate seismicity and tectonics of coastal northern California: Bull. Seis. Soc. America, v. 60.

Silver, E.A., Jan 1971, Transitional tectonics and late Cenozoic structure of the continental margin off northernmost California: Geol. Soc. America Bull., v. 82.

Silver, E.A., Nov. 1971, Tectonics of the Mendocino triple junction: Geol. Soc. America Bull., v. 82.

Tobin, D.G., and Sykes, L.R., 1968, Seismicity and tectonics of the northeast Pacific Ocean: Jour. Geophys. Research, v. 73.

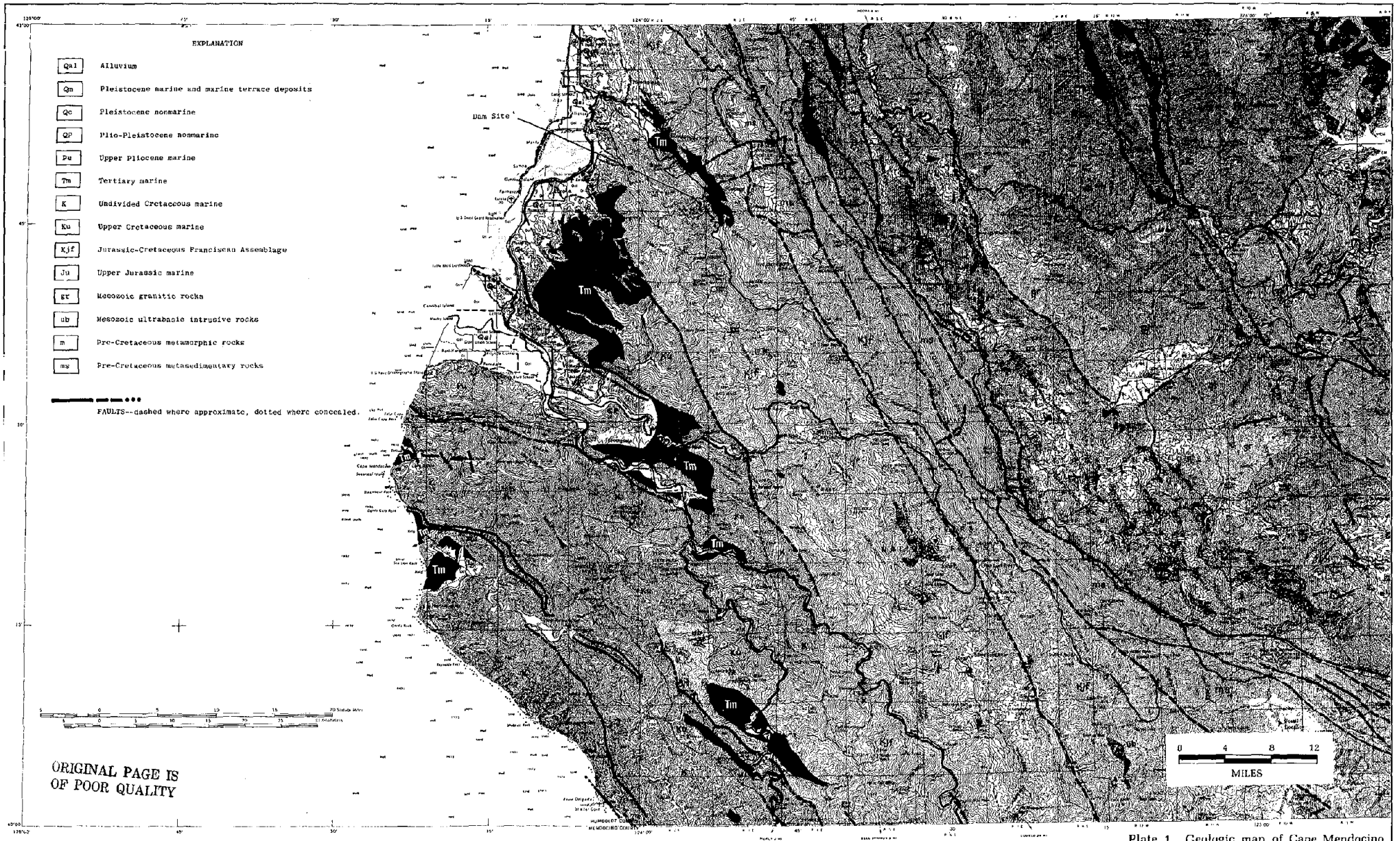

ORIGINAL PAGE IS
OF POOR QUALITY

PRECEDING PAGE BLANK NOT FILMED

FOLDOUT FRAME 1

Plate 1. Geologic map of Cape Mendocino area covering most of the study area; from State of California, Redding Sheet (1962).

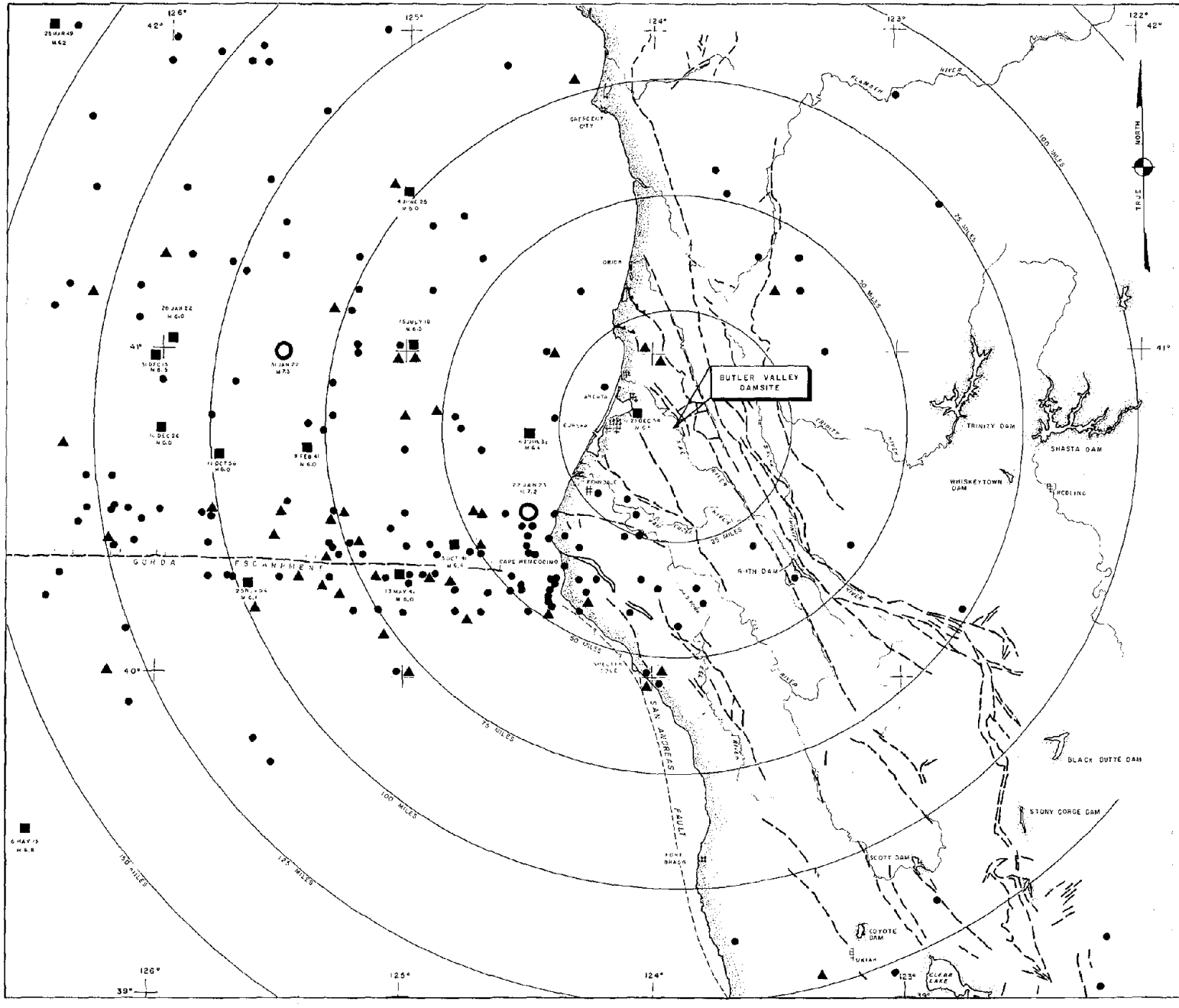

EXPLANATION

- Mag. 4.0 – 4.9
- Mag. 5.0 – 5.9
- Mag. 6.0 – 6.9
- Mag. 7.0 – 7.9
- FAULT *(Approximate location)*

NOTE:

This plate shows only those epicenters of earthquakes having a Richter Magnitude of 4.0 or greater. These data are from the seismograph station, Department of Geology and Geophysics, University of California, Berkeley. The period of record is 1915 thru 1972. The record between 1915 and 1930 shows only those events with assigned magnitudes of 6.0 or greater. All epicenters of earthquakes of 4.0 or greater are shown for the period 1931 thru 1972.

8 0 8 16

GRAPHIC SCALE IN MILES

Plate 2. Earthquake epicenters

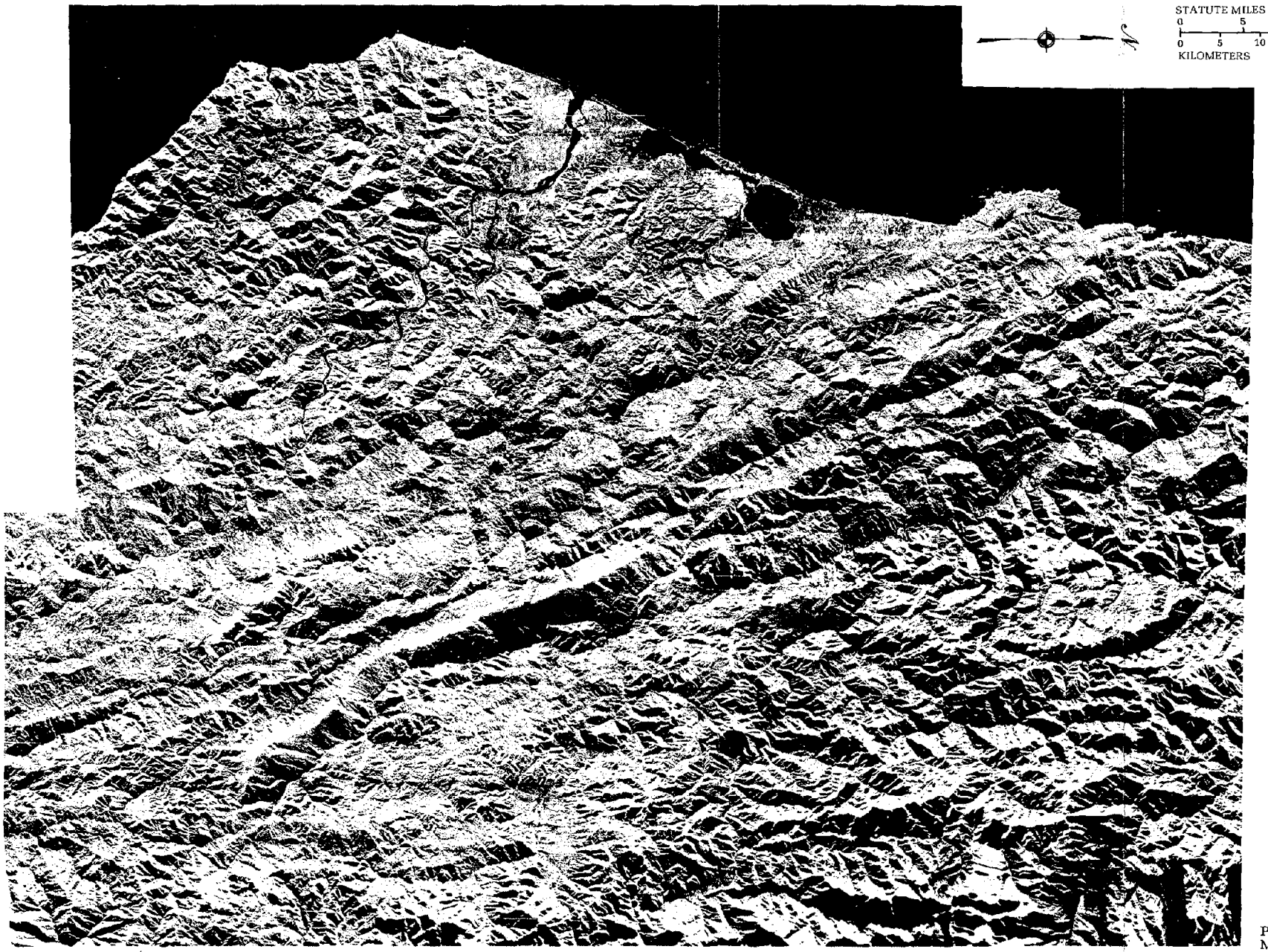

Plate 3. Radar mosaic, Cape Mendocino, California.

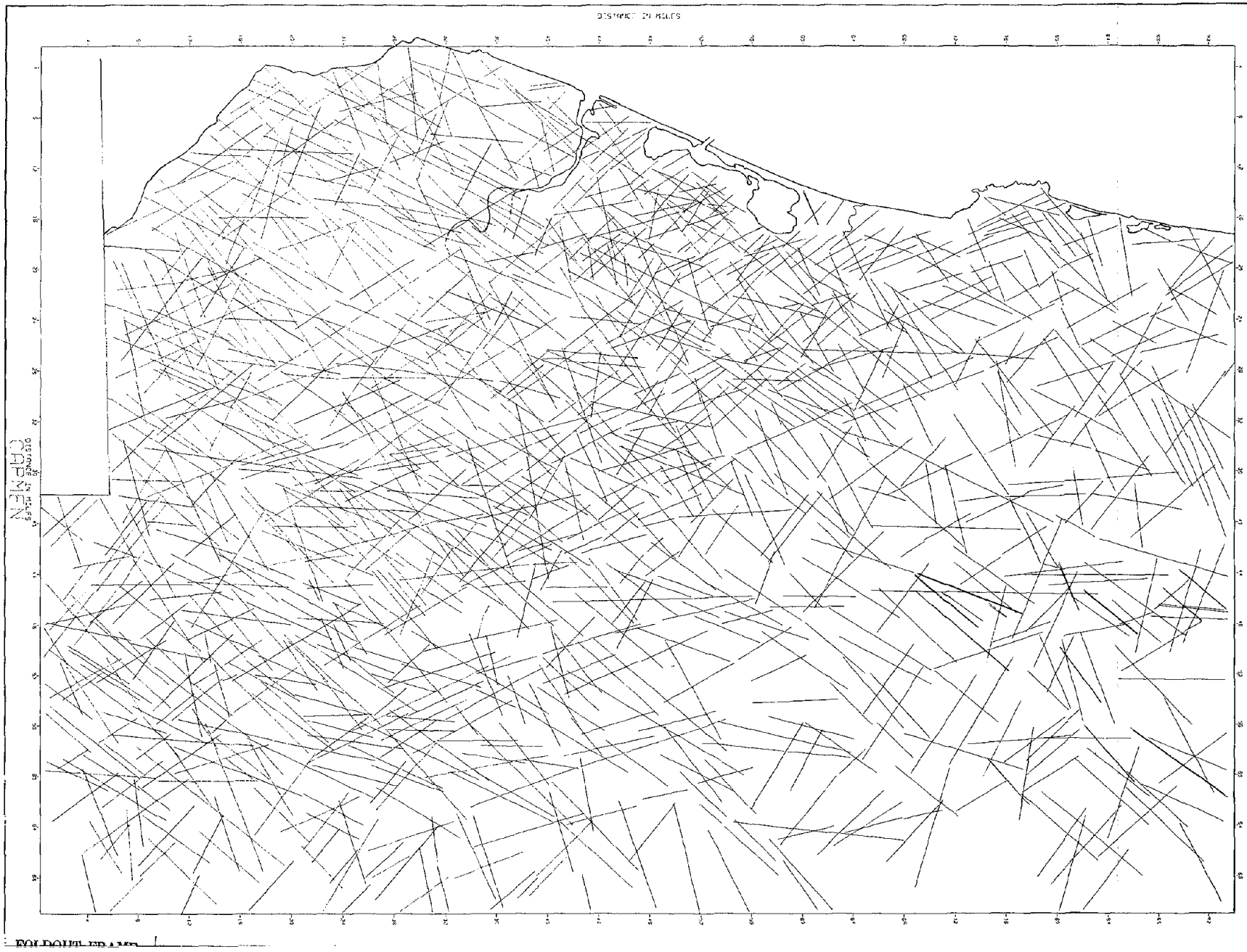

Plate 4. Principal lineaments interpreted from the Radar mosaic, plate 3.

FOLDOUT FRAME 3